mathematics

MDPI

Article

Decomposition of Complete, Complete Bipartite, and Complete Tripartite Graphs into Half-Sunlet Graphs of Order Twelve

Gajendran Palaniyandi [1,*], Aramuthakannan Soundararajan [1] and Sandhya Soundararajan [2]

[1] Department of Mathematics, PSG Institute of Technology and Applied Research, Coimbatore 641062, India; sakannan@psgitech.ac.in
[2] Department of IT and Operations, ICFAI Business School, Off-Campus Center of IFHE University, Bengaluru 560060, India; s.sandhya@ibsindia.org
* Correspondence: gajendranp@psgitech.ac.in

Abstract

The half-sunlet graph HS_{3k} is a $2k$-cycle with a pendant edge at every alternate vertex ($|V| = |E| = 3k$). We give a complete decomposition theory for HS_{12} ($k = 4$), characterising when HS_{12} decomposes G for G complete, complete bipartite, and complete tripartite. Writing $m = \min(a, b)$ and $M = \max(a, b)$, we prove the following. First, $HS_{12} \mid K_a$ if and only if $a \geq 16$ and $a \equiv 0, 1, 9, 16 \pmod{24}$. Second, $HS_{12} \mid K_{a,b}$ if and only if $m \geq 4$, $M \geq 8$ and 12 divides ab, with the single exception of the family in which $m = 6$, M is even and 3 does not divide M, for which no decomposition exists. Third, $HS_{12} \mid K_{a,b,c}$ if and only if 12 divides $ab + bc + ca$ and the multiset $\{a, b, c\}$ is none of $\{2, 2, c\}$, $\{1, 4, c\}$ with $c \equiv 4 \pmod{12}$, $\{1, 6, 6\}$ and $\{2, 3, 6\}$. The three hosts thus exhibit a structural gradient: the complete graph admits a purely arithmetic criterion with no exceptions, whereas the bipartite and tripartite hosts admit one and four exceptional families, respectively.

Keywords: graph decomposition; half-sunlet graph; complete graph; complete bipartite graph; complete tripartite graph; biclique partition; constraint programming

MSC: 05C70; 05C51; 05C85; 05C15; 90C10

1. Introduction

Throughout, all graphs are finite and simple. Write C_k for the cycle on k vertices, K_a for the complete graph on a vertices, $K_{a,b}$ for the complete bipartite graph with parts of size a, b, and $K_{a,b,c}$ for the complete tripartite graph with parts of size a, b, c. Following standard terminology [1,2], a graph G is H-decomposable ($H \mid G$) if $E(G)$ admits a partition $E_1, \ldots, E_k$ with each $\langle E_i \rangle$ isomorphic to H; equivalently, $G = H \oplus \cdots \oplus H$. Deciding, for a fixed small graph H, exactly which members of a host family are H-decomposable is a classical organising question in combinatorial design theory, and complete bipartite and complete multipartite graphs are among its most studied host families. Cycle decompositions of complete and complete multipartite graphs have been settled in wide generality: from the Kirkman–Netto triangle decomposition [3–5], through Alspach–Gavlas [6] and Sajna [7] for cycles of a single fixed length, to Bryant–Horsley–Pettersson for cycles of arbitrary length [8]. A second classical strand decomposes into stars, paths, or trees [9–18], and a third decomposes into bicliques of unrestricted size, following Graham and Pollak's theorem that the biclique partition number of K_a is $a - 1$ [19].

Since this paper's host graphs are the complete, complete bipartite, and complete tripartite families, we single out that literature for closer review. On the bipartite side,

Check for updates

Academic Editor: Zhibin Du

Received: 10 August 2026
Revised: 29 August 2026
Accepted: 2 September 2026
Published: 15 September 2026

Copyright: © 2026 by the authors. Licensee MDPI, Basel, Switzerland. This article is an open access article distributed under the terms and conditions of the Creative Commons Attribution (CC BY) license.

Sotteau's theorem gives a complete characterisation of $C_{2k} \mid K_{a,b}$ [20], and Chou, Fu, and Huang settled the decomposition of $K_{a,b}$ into short cycles more generally, including mixed cycle lengths [21,22]. Path and star decompositions of $K_{a,b}$ have an extensive literature of their own: Tarsi characterised decompositions into simple paths [23]; Jeevadoss and Muthusamy settled the mixed path-and-cycle case [13]; Shyu gave necessary and sufficient conditions for paths and stars with equal edge counts [24]; and Lee, together with various coauthors, resolved several cycle-and-star and multidecomposition variants of $K_{a,b}$ [25,26]. Closer in spirit to this paper, sunlet and generalised-sun decompositions of complete bipartite graphs have their own dedicated strand: Anitha and Lekshmi first established N-sun decompositions of K_a, $K_{a,b}$, and Harary graphs [27,28], and Fu, Jhuang, Lin, and Sung, together with Fu, Huang, and Lin, gave a systematic existence theory for general k-sun systems and 5-sun systems [29,30].

On the tripartite side, the analogous cycle-decomposition literature is older and, for odd cycle lengths, still only partially resolved. Cavenagh gave necessary and sufficient conditions for $C_k \mid K_{a,b,c}$ for several fixed k [31], and Billington settled the mixed case of cycles of length 3 and 4 [32]; Ganesamurthy and Paulraja later extended this to lengths 3 and 6 [33]. The *five*-cycle case, first posed by Mahmoodian and Mirzakhani [34], proved considerably harder and was advanced incrementally by Cavenagh and Billington [35] and by Alipour, Mahmoodian, and Mollaahmadi [36] with the general case remaining open when the three parts have pairwise distinct odd sizes. Path decompositions of complete tripartite graphs, and the mixed path-cycle problem specifically for paths and cycles of length three, were resolved by Priyadarsini, Shanmugasundaram, and Muthusamy [37]. Billington, Cavenagh, and Smith extended the path-and-cycle theory to complete *equipartite* graphs on three and five parts [38]. This paper's tripartite theory (Section 5) follows this same host family—complete tripartite graphs $K_{a,b,c}$—but for a fixed unicyclic target graph of order twelve rather than a bare cycle or path, and unlike the *five*-cycle problem above, we obtain a complete characterisation with no residual open cases.

We develop the complete, bipartite, and tripartite decomposition theory for HS_{12} from first principles. For the complete graph host, Theorem 6 gives an exception-free characterisation: $HS_{12} \mid K_a$ exactly when $a \geq 16$ and $a \equiv 0, 1, 9, 16 \pmod{24}$, which is proved by reducing every admissible order to four base cases via a recursive splitting that invokes the bipartite theorem as its bridge. For the multipartite hosts, we establish a complete bipartite characterisation and two tripartite master theorems that together cover every triple $a, b, c \geq 1$ with no exceptions beyond those explicitly identified: Theorem 9 resolves the entire domain $\min(a, b, c) \geq 8$ by a uniform divisibility criterion, and Theorem 12 resolves the remaining domain $\min(a, b, c) < 8$ via a finite reduction, uncovering two further infinite exceptional families along the way. The threshold 8 separating these two regimes is not a limitation of the method but a direct consequence of HS_{12}'s own bipartition structure, as discussed after Theorem 12 below. The novelty of these results is best stated against what is and is not already known. For the (full) sunlet graph L_{2m}, the existence of N-sun decompositions of complete and complete bipartite graphs is established [27–30] (Section 2.1), but no analogous complete characterisation—covering the complete, complete bipartite, and complete tripartite hosts together, with every exceptional case identified and proved rather than left open—exists for any half-sunlet graph prior to this paper for HS_{12} or otherwise. Not every result here required a new idea: the necessary conditions, peeling and bridging lemmas (Propositions 3 and Remark 8, Lemma 3), are deliberately elementary, exactly as such infrastructure is in the sunlet-decomposition literature above, and this is expected rather than a shortcoming: they are the bookkeeping on which the paper's substantive results are built. The genuinely novel contributions are four, and have no counterpart in the sunlet literature, precisely because L_{2m}'s symmetric bipartition (unlike

HS_{12}'s asymmetric $4+8$ split, Section 2.1) never produces the phenomena involved: the $K_{2,2,c}$ obstruction (Theorem 10), proved by an exhaustive colouring argument; the $K_{1,4,c}$ obstruction (Theorem 11), proved by an unrelated global degree-scheduling argument; the reduction theorem (Proposition 5) collapsing an infinite domain to a finite, fully resolved table, which is a technique that is not specific to HS_{12} and may transfer to other half-sunlet or unicyclic decomposition problems; and the complete-graph characterisation (Theorem 6), whose recursive reduction to four base cases uses the bipartite theorem of this paper as its bridge and yields, in contrast to every other host treated here, a characterisation with no exceptional families whatsoever. To verify the conditions and construct explicit decompositions, computational modelling was performed using the CP-SAT solver, which is a state-of-the-art constraint-programming and Boolean-satisfiability engine integrated within Google's OR-Tools suite [39]. CP-SAT lets us formulate exact partitioning rules, subgraph embedding constraints, and edge-disjointness requirements directly without the overhead of continuous relaxations, and it is the primary tool by which every sufficiency claim in this paper is established.

The paper is organised as follows. Section 2 fixes notation and records the structural facts about HS_{12} that the rest of the paper builds on. Section 3 proves the complete bipartite characterisation. Section 4 settles the complete-graph host K_a. Section 5 develops the tripartite hub method and the resulting master theorems, covering the entire domain $a, b, c \geq 1$. Section 7 records the computational methodology and verification procedure.

2. Preliminaries

2.1. Sunlet-Type Decomposition of Complete Graphs: Background and Structural Comparison

Decomposing the complete graph K_a into unicyclic "sun"-shaped target graphs is a classical strand of design theory alongside cycle and star decomposition. The (full) sunlet graph L_{2m} is the m-cycle $d_0 d_1 \cdots d_{m-1} d_0$ together with a pendant edge $d_i q_i$ at *every* cycle vertex d_i ($0 \leq i \leq m-1$), so $|V(L_{2m})| = |E(L_{2m})| = 2m$ and every cycle vertex has a degree of 3. For this target graph, the basic necessary condition for $L_{2m} \mid K_a$ is the usual edge-count divisibility $2m \mid \binom{a}{2}$ together with $a \geq m+1$ (enough vertices to supply both the m-cycle and its m distinct pendants); existence for complete and complete bipartite hosts under conditions of this type was established for general N-sun systems by Anitha and Lekshmi [27,28], and existence for K_a under the divisibility condition alone was settled for general k-sun systems by Fu, Jhuang, Lin, and Sung [29] with the *five*-sun case treated in full by Fu, Huang, and Lin [30]. This line of work remains active: Sonawane and Borse [40] settled the sunlet decomposition of hypercubes, and Sowndhariya and Muthusamy [41] resolved the sunlet decomposition of general product graphs both for sunlet graphs of order eight; Ezhilarasi and Muthusamy [42] extended path-and-cycle decomposition to complete equipartite hosts of arbitrary part count; Priyadarsini [43] extended the tripartite path-and-cycle results discussed above to paths of general length k; Arputha Jose, Sampath Kumar, and Cecily Sahai [44] settled the short-cycle (C_3, C_4, C_6)-decomposition of general complete tripartite graphs; Saranya, Jeevadoss, Nalini, and Chitra [45] extended the sunlet-adjacent hypercube decomposition programme to paths and cycles of general length; and Nalini et al. [46] settled the decomposition of regular bipartite graphs into Hamiltonian cycles or paths together with the star S_3.

The half-sunlet graph HS_{3k} studied in this paper differs from L_{2m} in one respect only—pendants at alternating cycle vertices rather than every cycle vertex—but this single change alters the decomposition theory qualitatively rather than incrementally. L_{2m} is edge-transitive under its own automorphism group in the relevant sense that every cycle vertex plays an identical role (degree 3, one pendant), so an embedding of L_{2m} into a bipartite host is governed by a single width parameter. HS_{3k}, by contrast, has two structurally distinct

vertex classes even before any embedding is chosen: the k pendant-bearing hubs (degree 3) and the $2k$ non-hub cycle and leaf vertices (degree 2 or 1), which are forced into different bipartition classes of sizes k and $2k$ by Remark 2. Consequently, as Lemma 2 makes precise below, embedding HS_{12} into $K_{a,b}$ requires two independent width thresholds, $m \geq 4$ and $M \geq 8$, rather than the single threshold that governs L_{2m}-decomposition. This two-parameter structure is the source of every exceptional family identified later in this paper (Theorems 5, 10 and 11), and it has no counterpart in the established sunlet-decomposition literature above, where the single-parameter symmetric structure of L_{2m} admits no analogous phenomenon.

It is worth noting where this asymmetry does not bite. The two-parameter width requirement is a statement about embedding HS_{12} into a graph whose vertex classes have prescribed, possibly unequal, sizes; the complete graph K_a imposes no such split, being vertex-transitive and $(a-1)$-regular. Accordingly, the complete-graph host behaves like the classical sunlet case rather than the multipartite one: Theorem 6 below shows $HS_{12} \mid K_a$ is governed by edge-count divisibility alone, with no exceptional family, exactly as k-sun systems of K_a are [29]. The contrast between this and the multipartite hosts, where exceptional families do arise, is one of the structural points this paper makes precise. The decomposition of complete graphs specifically into half-sunlet graphs remains comparatively unexplored in the literature; this paper's characterisation for HS_{12} across complete, complete bipartite, and complete tripartite hosts is offered as a step towards that broader theory.

2.2. General HS_{3k}: Structural Results Independent of k

Before specialising to $k = 4$, we record what can be established for the family HS_{3k} uniformly in k. The results of this subsection are proved once and used throughout the paper; they show that the framework developed here is a general one, and they isolate precisely which ingredients of the later analysis are k-independent and which are particular to $k = 4$.

Definition 1 (Half-sunlet graph)**.** *For $k \geq 3$, the* half-sunlet graph *HS_{3k} is the cycle $c_0c_1 \cdots c_{2k-1}c_0$ of length $2k$ together with k pendant edges $c_{2i}p_{2i}$ ($0 \leq i \leq k-1$) attached at the alternating vertices $c_0, c_2, \ldots, c_{2k-2}$, the leaves p_{2i} being distinct. Thus, $|V(HS_{3k})| = |E(HS_{3k})| = 3k$. We call the c_{2i} the* hubs *of HS_{3k}.*

Lemma 1 (Bipartition and degree sequence)**.** *For every $k \geq 3$, HS_{3k} is bipartite with classes*

$$P = \{c_0, c_2, \ldots, c_{2k-2}\}, \qquad Q = \{c_1, c_3, \ldots, c_{2k-1}\} \cup \{p_0, p_2, \ldots, p_{2k-2}\},$$

so that $|P| = k$ and $|Q| = 2k$. Every vertex of P has a degree of 3; of the $2k$ vertices of Q, exactly k have a degree of 2 and k have a degree of 1.

Proof. The cycle $c_0 \cdots c_{2k-1}$ has even length $2k$, so it is properly *two*-coloured by even- and odd-indexed vertices. Each pendant edge $c_{2i}p_{2i}$ joins an even-indexed vertex to a leaf, and placing every leaf in the odd class keeps the colouring proper; since leaves have no other neighbours, no conflict arises. Hence, $\{P, Q\}$ is a bipartition with $|P| = k$ even-indexed cycle vertices and $|Q| = k + k = 2k$. A hub c_{2i} meets two cycle edges and one pendant edge, so it has a degree of 3; a non-hub cycle vertex c_{2i+1} meets two cycle edges only, so has a degree of 2; a leaf has a degree of 1. □

The asymmetry $|P| = k \neq 2k = |Q|$ is the structural feature distinguishing HS_{3k} from the sunlet graph L_{2m}, whose two classes are of equal size, and it is the source of the width conditions that follow.

Corollary 1 (Embedding width). *If HS_{3k} embeds in $K_{a,b}$, then, writing $m = \min(a,b)$ and $M = \max(a,b)$,*

$$m \geq k \qquad \text{and} \qquad M \geq 2k.$$

Proof. $K_{a,b}$ has no edge inside a part, and HS_{3k} is connected, so its unique bipartition $\{P, Q\}$ of Lemma 1 must map with P inside one part and Q inside the other. Whichever part receives P has a size of at least $|P| = k$, and whichever receives Q has a size of at least $|Q| = 2k$; taking the better of the two orientations gives the stated bounds. □

Proposition 1 (Necessary conditions for the three host families). *Let $k \geq 3$. Then,*

$$HS_{3k} \mid K_{a,b} \implies 3k \mid ab, \tag{1}$$

$$HS_{3k} \mid K_{a,b,c} \implies 3k \mid (ab + bc + ca), \tag{2}$$

$$HS_{3k} \mid K_a \implies 6k \mid a(a-1) \text{ and } a \geq 3k. \tag{3}$$

Proof. Each copy of HS_{3k} contributes exactly $3k$ edges, so in every case, the number of edges of the host must be a multiple of $3k$. This gives (1) from $|E(K_{a,b})| = ab$ and (2) from $|E(K_{a,b,c})| = ab + bc + ca$. For (3), $|E(K_a)| = a(a-1)/2$, so $3k \mid a(a-1)/2$, i.e., $6k \mid a(a-1)$; and since HS_{3k} has $3k$ vertices, an embedding requires $a \geq 3k$. □

Proposition 2 (Hub-appearance bound). *Let $\mathcal{D}$ be an HS_{3k}-decomposition of a host G, and for $v \in V(G)$, let h_v denote the number of blocks of $\mathcal{D}$ in which v occupies a hub position. Then,*

$$h_v \leq \left\lfloor \frac{\deg_G(v)}{3} \right\rfloor \qquad \text{for every } v \in V(G),$$

independently of k.

Proof. By Lemma 1, a hub has a degree of 3 in HS_{3k} for every k, so each hub appearance of v consumes three distinct edges at v. Blocks of a decomposition are edge-disjoint, so the h_v hub appearances consume $3h_v$ distinct edges at v, whence $3h_v \leq \deg_G(v)$. □

Remark 1 (Scope of the general framework). *Three further ingredients of this paper are stated and proved for arbitrary k and are used unchanged in the sequel: the biclique-partition hub method (Definition 5), which refers only to the bipartition of Lemma 1; the peeling and bridging lemmas; and the complete-graph splitting $K_{a+b} = K_a \oplus K_b \oplus K_{a,b}$ used in Section 4, which is independent of the guest graph altogether. What is* not *k-independent is the resolution of the finitely many residue classes left open by Proposition 1: the base certificates, and hence the exceptional families, depend on the arithmetic of $3k$. For $k = 4$, the factorisation $12 = 4 \cdot 3$ governs the mod-4/mod-3 analysis of Section 5 and the residues $0, 1, 9, 16 \pmod{24}$ of Theorem 6. This paper carries the programme through in full for $k = 4$; the general framework above is what makes the comparison across k precise, and Section 8 records which further steps are expected to transfer.*

Definition 2 (The case $k = 4$). *HS_{12} is the case $k = 4$ of Definition 1: the 8-cycle $c_0c_1c_2c_3c_4c_5c_6c_7c_0$ together with four pendant edges c_0p_0, c_2p_2, c_4p_4, c_6p_6 at the hubs c_0, c_2, c_4, c_6 (see Figure 1), so $|V(HS_{12})| = |E(HS_{12})| = 12$ and, by Lemma 1, its bipartition classes have sizes 4 and 8.*

We record decompositions of HS_{12} inside a labelled host graph using the compact matrix notation

$$\begin{pmatrix} & p_0 & & p_2 & & p_4 & & p_6 & \\ c_0 & c_1 & c_2 & c_3 & c_4 & c_5 & c_6 & c_7 & c_0 \end{pmatrix}.$$

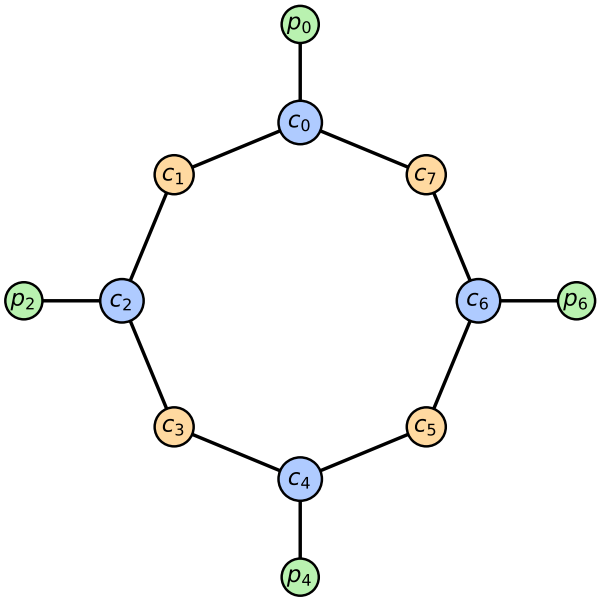


Figure 1. The half-sunlet graph HS_{12}.

Remark 2 (Bipartition of HS_{12})**.** *HS_{12} is bipartite with parts*

$$P = \{c_0, c_2, c_4, c_6\}, \qquad Q = \{c_1, c_3, c_5, c_7, p_0, p_2, p_4, p_6\},$$

$|P| = 4$, $|Q| = 8$, every edge, joining P to Q: the 8-cycle, is properly two-coloured by $\{c_0, c_2, c_4, c_6\}$ and $\{c_1, c_3, c_5, c_7\}$, and each pendant edge $c_i p_i$ forces its leaf into the class opposite c_i. Every vertex of P has a degree of 3 (two cycle edges plus one pendant edge); every vertex of Q has a degree of 2 (if a cycle vertex) or 1 (if a pendant leaf).

We call the four vertices of P (each of degree 3) the hubs of HS_{12} and the eight vertices of Q (degree 2 or 1) its non-hub vertices; the pendant edges attach a distinct leaf to each hub. This terminology is reused in a second and distinct sense—a chosen hub part among the three parts of $K_{a,b,c}$, rather than a hub vertex within HS_{12} itself—in Definition 5 below.

Definition 3 (Embedding)**.** *An embedding of a graph H into a graph G is an injective map $\phi : V(H) \to V(G)$ such that $uv \in E(H)$ implies $\phi(u)\phi(v) \in E(G)$ (a subgraph embedding, i.e., a graph monomorphism; ϕ need not be induced, and G may have edges between $\phi(u), \phi(v)$ for non-adjacent $u, v \in V(H)$ without affecting whether ϕ is an embedding). We write ϕ embeds H in G. Section 6 formalises the stronger, decomposition-specific notion of a block placement (Definition 7) needed for the certificate-based proofs later in this paper; every block placement is in particular an embedding in the sense defined here.*

Lemma 2 (Embedding requires widths 4 and 8)**.** *If ϕ embeds HS_{12} in $K_{a,b}$ with parts X ($|X| = a$), Y ($|Y| = b$), then either $\phi(P) \subseteq X$, $\phi(Q) \subseteq Y$, or $\phi(P) \subseteq Y$, $\phi(Q) \subseteq X$. Consequently, writing $m = \min(a, b)$, $M = \max(a, b)$, $m \geq 4$ and $M \geq 8$ are necessary for any embedding of HS_{12} into $K_{a,b}$.*

Proof. $K_{a,b}$ has no edges inside either part, and HS_{12} is connected with the unique bipartition $\{P, Q\}$ of Remark 2, so $\phi(P)$ lies entirely in X or Y, and $\phi(Q)$ lies in the other. Since $|P| = 4$, $|Q| = 8$, whichever side receives P needs a size ≥ 4 and whichever receives Q needs a size ≥ 8; the better orientation gives $m \geq 4$, $M \geq 8$. □

For disjoint vertex sets S, T, write $K_{S,T}$ for the complete bipartite graph with parts S, T. A biclique is a complete bipartite graph; a biclique subgraph of a graph G is a subgraph of G isomorphic to $K_{S,T}$ for some disjoint $S, T \subseteq V(G)$.

Definition 4 (Biclique partition). *A biclique partition of a graph G is a finite collection of biclique subgraphs of G whose edge sets partition $E(G)$.*

Write the three parts of $K_{a,b,c}$ as X, Y, Z, of sizes a, b, c, respectively; WLOG we may assume $a \leq b \leq c$ whenever convenient below.

Definition 5 (Hub condition). *For a hub part $H \in \{X, Y, Z\}$ with the other two parts Q, R, the hub-H condition holds if both $HS_{12} \mid K_{|H|,|Q|+|R|}$ and $HS_{12} \mid K_{|Q|,|R|}$, which are each decided by Theorem 5.*

3. HS_{12}-Decomposition of $K_{a,b}$

Proposition 3 (Necessary condition). *If $HS_{12} \mid K_{a,b}$, then $12 \mid ab$.*

Proof. $|E(K_{a,b})| = ab$ and each HS_{12}-copy has 12 edges, so a decomposition into t copies forces $ab = 12t$. □

Definition 6 (Edge-disjoint union $\oplus$ [47]). *For graphs $G_1, \ldots, G_r$, the notation $G = G_1 \oplus \cdots \oplus G_r$ means that $V(G) = V(G_1) \cup \cdots \cup V(G_r)$ and $E(G)$ is partitioned by $E(G_1), \ldots, E(G_r)$, i.e., the $E(G_i)$ are pairwise edge-disjoint and their union is exactly $E(G)$. Equivalently, $G_1 \oplus \cdots \oplus G_r$ is the graph obtained by taking the union of the G_i on their combined vertex set and superimposing their edge sets without identifying or duplicating any edge.*

Lemma 3. *For any $a, b \geq 1$ and any splitting $b = b_1 + b_2$ with $b_1, b_2 \geq 0$,*

$$K_{a,b} = K_{a,b_1} \oplus K_{a,b_2},$$

the second summand being the complete bipartite graph between the a-side and the peeled block of size b_2. The analogous splitting holds on the a-side.

Proof. Partition the b-side into blocks of size b_1, b_2. Every edge of $K_{a,b}$ has its b-side endpoint in exactly one of the two blocks; this partitions $E(K_{a,b})$ into $E(K_{a,b_1})$ and $E(K_{a,b_2})$ exactly. □

Corollary 2. *If $HS_{12} \mid K_{a,b}$ and $HS_{12} \mid K_{a,b'}$, then $HS_{12} \mid K_{a,b+b'}$. The analogous statement holds on the a-side.*

Lemma 2 shows $m = \min(a, b) \geq 4$, $M = \max(a, b) \geq 8$ are necessary for any embedding at all. Because $|P| = 4 \neq 8 = |Q|$, the two bipartition classes have different widths, and this asymmetry produces a forced-orientation phenomenon over an entire range of small values $4 \leq a < 8$ rather than at a single isolated boundary point: any graph whose two bipartition classes were instead of equal size would only see this phenomenon exactly at the shared width value, since below it neither orientation is ruled out by a width mismatch.

Theorem 1. *Suppose $HS_{12} \mid K_{a,b}$ with $4 \leq a < 8 \leq b$. Then, every copy of HS_{12} in the decomposition has P embedded in the a-side and Q in the b-side; consequently, $3 \mid b$.*

Proof. By Lemma 2, each copy's embedding orientation requires either (P-side ≥ 4 and Q-side ≥ 8) or (P-side ≥ 8 and Q-side ≥ 4). Since $a < 8$, the a-side cannot host Q (which needs ≥ 8), so every copy must embed P in the a-side and Q in the b-side. Fix x in the a-side, and let $t(x)$ be the number of copies containing x. In every one of those copies, x plays a P-role vertex, which by Remark 2 has a degree of exactly 3. Hence, $\deg_{K_{a,b}}(x) = b = 3\,t(x)$, forcing $3 \mid b$. □

Theorem 2. *For $b \geq 8$, $HS_{12} \mid K_{6,b}$ if and only if $6 \mid b$.*

Proof. (Necessity) By Proposition 3, $12 \mid 6b$, i.e., $2 \mid b$. By Theorem 1 (applicable since $6 < 8 \leq b$), $3 \mid b$. Together, $6 \mid b$.

(Sufficiency) The base cases $K_{6,12}$ and $K_{6,18}$ (one representative of each residue of b modulo 6 that is $\equiv 0 \pmod 6$, restricted to $b \geq 12$; the smallest admissible value, $b = 6$ itself, is excluded by the hypothesis $b \geq 8$) are exhibited explicitly in Appendix A and independently re-verified. For general $b \geq 12$ with $6 \mid b$: writing $b = 12i + 18j$ with $i, j \geq 0$ (possible for every multiple of 6 that is $\geq$12, since $\{2, 3\}$—the coefficients of 12, 18 in units of 6—are coprime with Frobenius number 1, and $12/6 = 2$, $18/6 = 3$ already cover every integer $k \geq 2$ as a non-negative combination of 2 and 3), Corollary 2 applied $i + j - 1$ times, bridging with $K_{6,12}$ (see Figure 2) and $K_{6,18}$ (see Figure 3) as needed, gives $HS_{12} \mid K_{6,b}$. □

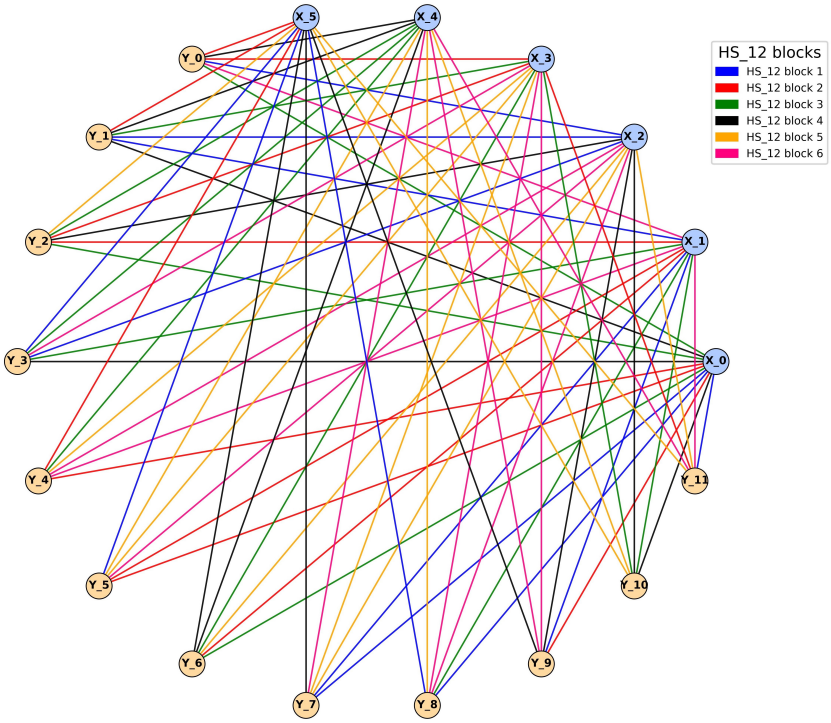


Figure 2. HS_{12}-decomposition of $K_{6,12}$.

Corollary 3. *For $b \geq 8$ even with $3 \nmid b$ (equivalently, $b \equiv 2$ or $4 \pmod 6$), $HS_{12} \nmid K_{6,b}$, even though $12 \mid 6b$.*

Proof. Since b is even and $3 \nmid b$, we have $6 \nmid b$ (as $6 \mid b$ would force $3 \mid b$). By Theorem 2, $HS_{12} \mid K_{6,b}$ holds if and only if $6 \mid b$; since $6 \nmid b$, $HS_{12} \nmid K_{6,b}$. □

We next show that $a = 6$ is the *only* value in $\{4, 5, 6, 7\}$ at which this gap between $12 \mid ab$ and the forced condition $3 \mid b$ can occur.

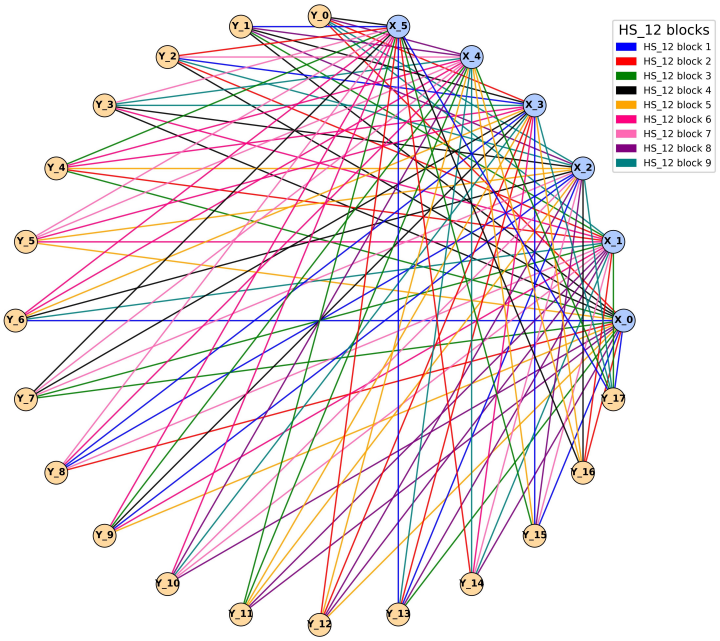


Figure 3. HS_{12}-decomposition of $K_{6,18}$.

Remark 3. *For $a \in \{4,5,7\}$ and $b \geq 8$, $12 \mid ab$ implies $3 \mid b$, and it adds no restriction beyond $12 \mid ab$ itself. For $a = 4$: $12 \mid 4b \iff 3 \mid b$ directly. For $a = 5,7$: $\gcd(a,12) = 1$, so $12 \mid ab \iff 12 \mid b$, which implies $3 \mid b$.*

Lemma 4. *Each of $K_{4,9}$, $K_{4,12}$, $K_{4,15}$, $K_{5,12}$, $K_{6,12}$, $K_{6,18}$, and $K_{7,12}$ is HS_{12}-decomposable. Explicit certificates, each found by CP-SAT and independently re-verified edge-by-edge, are given in Appendix A.*

Proof. The existence of an HS_{12}-decomposition is, by definition, the existence of an explicit finite collection of edge-disjoint HS_{12}-copies whose union is the full edge set; exhibiting such a collection *is* the proof regardless of whether it was found by hand or by computer search. Each certificate here was found by CP-SAT (a constraint solver that returns an exact satisfying assignment rather than an approximation or a heuristic guess) and then independently re-verified by a separate program, sharing no code with the solver, that reconstructs every block's twelve edges from the raw certificate and checks by direct enumeration that the blocks are pairwise edge-disjoint and that their union is exactly $E(K_{a,b})$—exactly the definition of a decomposition, which is checked mechanically rather than asserted.

As an explicit illustration, $K_{4,9}$ ($ab = 36 = 3 \times 12$) is decomposed by the three blocks

$$H_1 = \begin{pmatrix} & Y_3 & & Y_5 & & Y_7 & & Y_2 & \\ X_0 & Y_0 & X_1 & Y_1 & X_2 & Y_6 & X_3 & Y_8 & X_0 \end{pmatrix},$$

$$H_2 = \begin{pmatrix} & Y_6 & & Y_3 & & Y_2 & & Y_8 & \\ X_0 & Y_1 & X_3 & Y_5 & X_2 & Y_4 & X_1 & Y_7 & X_0 \end{pmatrix},$$

$$H_3 = \begin{pmatrix} & Y_5 & & Y_6 & & Y_8 & & Y_7 & \\ X_0 & Y_2 & X_1 & Y_3 & X_2 & Y_0 & X_3 & Y_4 & X_0 \end{pmatrix}.$$

A direct hand count confirms these $3 \times 12 = 36$ edges are pairwise distinct and exhaust $E(K_{4,9})$: each X_i ($i = 0, \ldots, 3$) meets every Y_j ($j = 0, \ldots, 8$) in exactly one block.

The remaining six certificates ($K_{4,12}$, $K_{4,15}$, $K_{5,12}$, $K_{6,12}$, $K_{6,18}$, $K_{7,12}$) are of the identical explicit, hand-checkable form and are given in full in Appendix A. □

Theorem 3 (Complete resolution for $a \in \{4,5,7\}$)**.** *For $a \in \{4,5,7\}$ and $b \geq 8$, $HS_{12} \mid K_{a,b}$ if and only if $12 \mid ab$.*

Proof. Necessity combines Theorem 1 and Remark 3. For sufficiency at $a = 5,7$: by Lemma 4, $K_{5,12}$ and $K_{7,12}$ are each verified; since the feasible b values are exactly the multiples of 12 that are ≥ 12 (as $12 \mid ab$ with $\gcd(a,12) = 1$ forces $12 \mid b$), every feasible b is $b = 12k$ for $k \geq 1$, and Corollary 2 applied $k-1$ times using the $K_{a,12}$ certificate gives $HS_{12} \mid K_{a,b}$. For $a = 4$, the feasible b values are exactly $\{b \geq 8 : 3 \mid b\} = \{9, 12, 15, 18, 21, \dots\}$. By Lemma 4, $K_{4,9}$, $K_{4,12}$, and $K_{4,15}$ are verified. Writing $b = 9i + 12j + 15\ell$ with $i, j, \ell \geq 0$: since $\{3,4,5\}$ (the coefficients of $9, 12, 15$ in units of 3) generate every integer ≥ 3 as a non-negative combination—$3, 4, 5$ themselves, then $6 = 3+3$, $7 = 3+4$, $8 = 4+4$, and every $k \geq 6$ by adding 3's to a representative of k mod $3 \in \{6,7,8\}$—every $b \in \{9, 12, 15, 18, \dots\}$ is such a combination, and Corollary 2 applied repeatedly, bridging with whichever of $K_{4,9}, K_{4,12}, K_{4,15}$ is needed at each step, gives $HS_{12} \mid K_{4,b}$. □

Remark 4. *Combined with Theorem 2 ($a = 6$), this resolves $HS_{12} \mid K_{a,b}$ for every $a \in \{4,5,6,7\}$, $b \geq 8$.*

The Free Regime $a, b \geq 8$

Once both sides have a width ≥ 8, a block may choose *either* orientation—P in the a-side or P in the b-side—since both sides now satisfy the mild bound (≥ 4) as well as the strict bound (≥ 8). We show this restores full flexibility: the forced-orientation gap of Theorem 1 disappears entirely, and the two regimes (forced below width 8, free at or above it) sit as different chapters of the same theorem.

Lemma 5. *Assume $a, b \geq 8$ and $12 \mid ab$. Then, at least one of a, b is divisible by 3.*

Proof. Since $12 = 4 \times 3 \mid ab$, we have $3 \mid ab$, hence (as 3 is prime) $3 \mid a$ or $3 \mid b$; pick either side with this property as the Q-side. Running a single-orientation construction with Q fixed on that side requires only the following: that side ≥ 8 (true, as both $a, b \geq 8$) and 3 divides it (true by choice); the complementary P-side needs only ≥ 4, which holds automatically since $a, b \geq 8 \geq 4$. □

Fix such a side and call it the Q-side for a single-orientation construction (every block places Q there, P on the other side). This choice is available for both sides in general—a genuine choice, not a further restriction—and, if the chosen Q-side is b, then say that Theorem 1's degree argument, run in reverse with the roles of P, Q exchanged, requires no condition on a at all beyond $a \geq 4$ (satisfied since $a \geq 8$). Consequently, whenever $a, b \geq 8$ and $12 \mid ab$, some single orientation is arithmetically eligible; the remaining question is purely combinatorial existence, which is resolved by the following base cases.

Lemma 6 (Verified base decompositions, free regime)**.** *Each of $K_{9,16}$ and $K_{15,16}$ is HS_{12}-decomposable.*

Proof. Split the size-16 side into four blocks of size 4: $16 = 4+4+4+4$. By Lemma 4, $K_{4,9}$ is HS_{12}-decomposable; applying the a-side bridge of Corollary 2 three times to four disjoint copies of this decomposition, one per block, gives

$$K_{16,9} = K_{4,9} \oplus K_{4,9} \oplus K_{4,9} \oplus K_{4,9},$$

each summand an independent copy of the certificate already exhibited and verified in the proof of Lemma 4, on its own disjoint set of *four* vertices from the size-16 side and the shared size-9 side. The identical argument, using $K_{4,15}$ in place of $K_{4,9}$, gives $K_{16,15} = K_{4,15} \oplus K_{4,15} \oplus K_{4,15} \oplus K_{4,15}$. Both constructions are thus explicit and hand-checkable given the base certificate already reproduced above with no further computation required. □

Theorem 4. *For $a, b \geq 8$, $HS_{12} \mid K_{a,b}$ if and only if $12 \mid ab$.*

Proof. The necessity is Proposition 3. For sufficiency, let a_0, b_0 be the representatives of $a, b \pmod{12}$ lying in $\{8, \ldots, 19\}$. Writing $a = a_0 + 12i$, $b = b_0 + 12j$ for $i, j \geq 0$, one checks $ab \equiv a_0 b_0 \pmod{12}$, so $12 \mid ab \iff 12 \mid a_0 b_0$; it therefore suffices to resolve every representative pair (a_0, b_0) with $8 \leq a_0 \leq b_0 \leq 19$ and $12 \mid a_0 b_0$—there are exactly 21 such pairs—and then bridge.

For the bridging step: by Theorem 3 and Lemma 4, $HS_{12} \mid K_{r,12}$ for $r \in \{4, 5, 6, 7\}$; writing any $x \geq 4$ as $x = r + 4k$ with $r \in \{4, 5, 6, 7\}$, $k \geq 0$, and applying Lemma 3 to split the x-side into a block of size r and k blocks of size 4 gives $HS_{12} \mid K_{x,12}$ for every integer $x \geq 4$; by symmetry, the same holds for $K_{12,x}$. Corollary 2 then lets us grow either side of any verified pair by 12 at a time without further hypotheses on the other side beyond ≥ 4.

For the 21 representative pairs themselves: twelve involve $a_0 = 12$ or $b_0 = 12$ and are resolved directly by the universal fact just proved. Of the remaining nine, $(8, 9)$, $(8, 15)$, $(8, 18)$, $(10, 18)$, $(14, 18)$, $(16, 18)$, and $(18, 18)$ are each obtained for free by Lemma 3, splitting one side into parts of size 4 and/or 6 and combining already established pieces $K_{4,9}$, $K_{4,15}$, $K_{4,18}$ ($= K_{4,9} \oplus K_{4,9}$, itself free), and $K_{6,18}$; for instance, $K_{8,18} = K_{4,18} \oplus K_{4,18}$, $K_{14,18} = K_{8,18} \oplus K_{6,18}$, and $K_{18,18} = K_{4,18} \oplus K_{4,18} \oplus K_{6,18} \oplus K_{4,18}$. The final two, $(9, 16)$ and $(15, 16)$ (see Figure 4), are resolved by the direct certificates of Lemma 6. This exhausts all 21 representative pairs. □

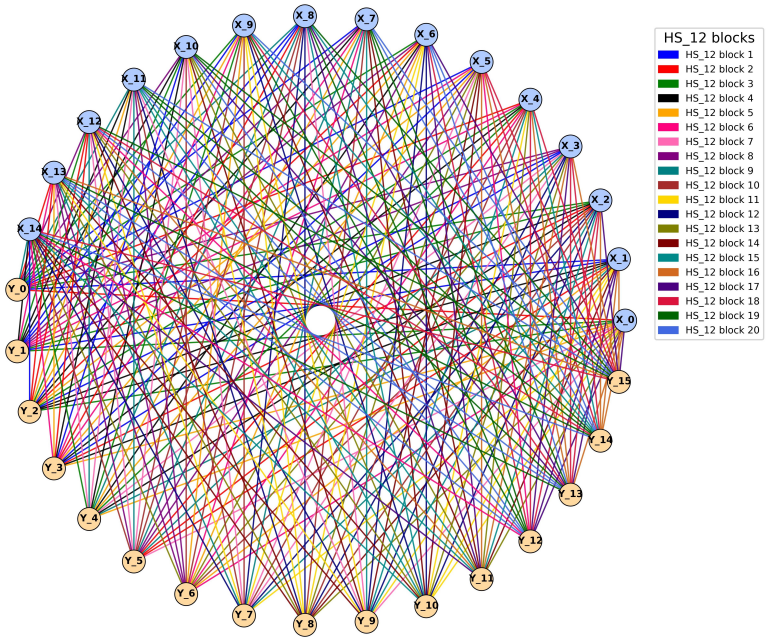


Figure 4. HS_{12}-decomposition of $K_{15,16}$.

Theorem 5. *Let $a, b \geq 1$, $m = \min(a, b)$, $M = \max(a, b)$. Then, $HS_{12} \mid K_{a,b}$ if and only if all of the following hold:*

(i) *$m \geq 4$ and $M \geq 8$;*

(ii) $12 \mid ab$;
(iii) *It is not the case that* $m = 6$ *and* M *is even with* $3 \nmid M$.

Proof. The necessity of (i) is Lemma 2; of (ii) is Proposition 3; of (iii) is Corollary 3. For sufficiency: if $m < 8$, then $m \in \{4, 5, 6, 7\}$ by (i), and the claim is Theorem 3 (condition (iii) restricting exactly the $m = 6$ sub-case, which is vacuous for $m \in \{4, 5, 7\}$ by Remark 3). If $m \geq 8$, the claim is that Theorem 4 (condition (iii) is automatically vacuous, since it requires $m = 6 < 8$). □

4. HS_{12}-Decomposition of K_a

This section settles the complete-graph host case. The characterisation is obtained from two ingredients: an elementary arithmetic necessary condition and a recursive construction that reduces every admissible order to four base cases.

4.1. Necessary Conditions

Proposition 4 (Necessary condition). *If* $HS_{12} \mid K_a$, *then* $a \geq 12$ *and* $24 \mid a(a-1)$; *equivalently,* $a \geq 16$ *and*

$$a \equiv 0,\ 1,\ 9,\ \text{or } 16 \pmod{24}.$$

Proof. Since HS_{12} has twelve vertices, an embedding requires $a \geq 12$. Each copy of HS_{12} contributes exactly 12 edges and $|E(K_a)| = \binom{a}{2} = a(a-1)/2$, so a decomposition into t copies forces $a(a-1)/2 = 12t$, i.e., $24 \mid a(a-1)$.

For the residue form, write $24 = 8 \cdot 3$. Since a and $a-1$ are coprime, $8 \mid a(a-1)$ forces $8 \mid a$ or $8 \mid a-1$, and $3 \mid a(a-1)$ forces $3 \mid a$ or $3 \mid a-1$. Combining the four cases by the Chinese Remainder Theorem gives $a \equiv 0, 1, 9, 16 \pmod{24}$. Finally, $a \equiv 0, 1, 9, 16 \pmod{24}$ together with $a \geq 12$ excludes $a = 12$ (as $12 \cdot 11 = 132$ is not divisible by 24) and leaves $a \geq 16$. □

Remark 5. *Unlike the bipartite host case, no degree obstruction arises here. Every vertex of* K_a *has the same degree* $a-1$, *and* HS_{12} *supplies vertices of degree 3, 2, and 1; since* $\gcd(3, 2, 1) = 1$, *any degree budget* $a-1$ *admits a representation* $3h + 2n + \ell$ *with* $h, n, \ell \geq 0$. *The arithmetic condition of Proposition 4 is therefore the only local obstruction.*

4.2. A Recursive Construction

The following splitting is the complete-graph analogue of the peel-and-bridge Lemma 3, and it is what allows an infinite family to be reduced to finitely many base cases.

Lemma 7 (Complete-graph splitting). *For any* $a, b \geq 1$,

$$K_{a+b} = K_a \oplus K_b \oplus K_{a,b},$$

in the sense of Definition 6.

Proof. Partition $V(K_{a+b})$ into disjoint sets A and B with $|A| = a$, $|B| = b$. Every edge of K_{a+b} has both endpoints in A, both endpoints in B, or one endpoint in each; these three cases are mutually exclusive and exhaust $E(K_{a+b})$, and the induced subgraphs are precisely K_a, K_b, and $K_{a,b}$. □

Corollary 4 (Recursive bridge). *If* $HS_{12} \mid K_a$, $HS_{12} \mid K_b$, *and* $HS_{12} \mid K_{a,b}$, *then* $HS_{12} \mid K_{a+b}$.

Proof. The following is immediate from Lemma 7: concatenating the three decompositions yields a set of edge-disjoint HS_{12}-copies whose union is exactly $E(K_{a+b})$. □

Because the middle term $K_{a,b}$ is governed by the complete bipartite characterisation already established in Theorem 5, Corollary 4 converts the complete-graph problem into a purely arithmetic reachability question.

4.3. Base Cases

Lemma 8 (Verified base decompositions)**.** *Each of K_{16}, K_{24}, K_{25}, and K_{33} is HS_{12}-decomposable into 10, 23, 25, and 44 blocks, respectively.*

Proof. As in Lemma 4, the proof consists of exhibiting an explicit collection of edge-disjoint HS_{12}-copies whose union is the full edge set; this is the definition of a decomposition, and exhibiting one *is* the proof. Each certificate was produced by the CP-SAT model of Section 7 and independently re-verified by a separate routine, sharing no code with the solver, which reconstructs every block's twelve edges and confirms pairwise edge-disjointness together with the exact coverage of $E(K_a)$.

The smallest instance, K_{16} (with $\binom{16}{2} = 120 = 10 \times 12$ edges), is decomposed by the ten blocks below, which is written in the matrix notation of Definition 2 with v_i denoting the i-th vertex of K_{16} (0-indexed):

$$H_1 = \begin{pmatrix} & v_3 & & v_{15} & & v_2 & & v_{13} & \\ v_0 & v_4 & v_{14} & v_{10} & v_{11} & v_{12} & v_9 & v_1 & v_0 \end{pmatrix},$$

$$H_2 = \begin{pmatrix} & v_{14} & & v_{15} & & v_4 & & v_{13} & \\ v_{11} & v_0 & v_9 & v_2 & v_8 & v_7 & v_{12} & v_5 & v_{11} \end{pmatrix},$$

$$H_3 = \begin{pmatrix} & v_{15} & & v_8 & & v_{11} & & v_7 & \\ v_{13} & v_6 & v_3 & v_4 & v_1 & v_{14} & v_0 & v_2 & v_{13} \end{pmatrix},$$

$$H_4 = \begin{pmatrix} & v_{15} & & v_9 & & v_7 & & v_2 & \\ v_8 & v_0 & v_6 & v_{14} & v_3 & v_{11} & v_4 & v_{12} & v_8 \end{pmatrix},$$

$$H_5 = \begin{pmatrix} & v_9 & & v_{10} & & v_{12} & & v_{13} & \\ v_{11} & v_8 & v_5 & v_6 & v_{15} & v_2 & v_{14} & v_7 & v_{11} \end{pmatrix},$$

$$H_6 = \begin{pmatrix} & v_{11} & & v_{10} & & v_1 & & v_9 & \\ v_{15} & v_3 & v_{13} & v_7 & v_6 & v_8 & v_{14} & v_5 & v_{15} \end{pmatrix},$$

$$H_7 = \begin{pmatrix} & v_{15} & & v_{11} & & v_2 & & v_7 & \\ v_{10} & v_8 & v_{13} & v_1 & v_{12} & v_3 & v_5 & v_4 & v_{10} \end{pmatrix},$$

$$H_8 = \begin{pmatrix} & v_{11} & & v_{15} & & v_0 & & v_2 & \\ v_6 & v_4 & v_7 & v_1 & v_5 & v_9 & v_3 & v_{10} & v_6 \end{pmatrix},$$

$$H_9 = \begin{pmatrix} & v_3 & & v_7 & & v_5 & & v_{12} & \\ v_1 & v_8 & v_9 & v_4 & v_{13} & v_0 & v_{10} & v_2 & v_1 \end{pmatrix},$$

$$H_{10} = \begin{pmatrix} & v_{14} & & v_5 & & v_9 & & v_4 & \\ v_{12} & v_6 & v_2 & v_7 & v_{10} & v_1 & v_{15} & v_0 & v_{12} \end{pmatrix}.$$

A direct count confirms that these $10 \times 12 = 120$ edges are pairwise distinct and exhaust $E(K_{16})$. The certificates for K_{24}, K_{25}, and K_{33} are of the identical explicit form and are given in full in the Supplementary Information. □

4.4. The Master Theorem

Theorem 6 (Complete characterisation for K_a)**.** *For every integer $a \geq 1$,*

$$HS_{12} \mid K_a \iff a \geq 16 \text{ and } a \equiv 0, 1, 9, 16 \pmod{24}.$$

Proof. The necessity is Proposition 4.

For sufficiency, we induct on a. The four smallest admissible orders, $a = 16, 24, 25, 33$, are Lemma 8. Let $a \geq 40$ be admissible and suppose every admissible order smaller than a is HS_{12}-decomposable. Choose $r \in \{16, 24, 25, 33\}$ according to the residue of a:

$$r = \begin{cases} 24, & a \equiv 0 \pmod{24}, \\ 25, & a \equiv 1 \pmod{24}, \\ 33, & a \equiv 9 \pmod{24}, \\ 16, & a \equiv 16 \pmod{24}, \end{cases}$$

and set $c = a - r$. In each case, $r \equiv a \pmod{24}$, so $24 \mid c$; hence, $c \equiv 0 \pmod{24}$ is admissible, and $c \geq 16$ because $a \geq 40$ and $c = a - r$ is a positive multiple of 24. By the induction hypothesis $HS_{12} \mid K_c$, and $HS_{12} \mid K_r$ by Lemma 8.

It remains to check $HS_{12} \mid K_{r,c}$ via Theorem 5. In every case, $\min(r, c) \geq 16 > 6$, so the exceptional family at $\min = 6$ is vacuous, and $\min(r, c) \geq 4$, $\max(r, c) \geq 8$ hold. The divisibility $12 \mid rc$ holds in each case because $24 \mid c$:

- $r = 24$ or $r = 16$: $12 \mid rc$ since $12 \mid 24 \mid c$;
- $r = 25$: $\gcd(25, 12) = 1$, and $12 \mid c$, so $12 \mid 25c$;
- $r = 33$: $33c = 3 \cdot 11 \cdot c$ and $4 \mid 24 \mid c$, so $12 \mid 33c$.

Hence, $HS_{12} \mid K_{r,c}$, and Corollary 4 gives $HS_{12} \mid K_a = K_{r+c}$. The two remaining orders below the induction threshold, $a = 40 = 16 + 24$ and $a = 48 = 24 + 24$, follow directly from Corollary 4 together with Theorem 5 (as $12 \mid 16 \cdot 24$ and $12 \mid 24 \cdot 24$). □

Remark 6. *The complete-graph case is thus exception-free: unlike the bipartite host ($m = 6$) and the tripartite host ($K_{2,2,c}$, $K_{1,4,c}$, $K_{1,6,6}$, $K_{2,3,6}$), no admissible order fails. The structural reason is the one noted after Proposition 4: K_a is vertex-transitive and regular, so the width and degree-scheduling obstructions that drive the exceptional families elsewhere in this paper cannot arise, and the sole constraint is arithmetic.*

5. HS_{12}-Decomposition of $K_{a,b,c}$

Remark 7. *This section reuses several single-letter symbols with meanings local to the subsection in which they appear; the Table 1 below fixes each one's scope to help a reader carry the correct meaning forward.*

Table 1. Notation used in $HS_{12} \mid K_{a,b,c}$

Symbol	Meaning (Scope)
a, b, c	sizes of the three parts of $K_{a,b,c}$ (throughout)
t	number of HS_{12}-blocks in a decomposition, $t = (ab + bc + ca)/12$ (throughout)
m, M	$\min(a, b)$, $\max(a, b)$—*only* in Section 3's bipartite theory; re-purposed in Section 5.5 as the residue-family index $c = 12m + 4$
A, B, C	the three parts of $K_{a,b,c}$, treated as vertex colours (Section 5.4 onward whenever a hub-method or colouring argument is used)
v_0	the unique vertex of a singleton part ($a = 1$), Sections 5.5 and 5.6 only
D	v_0's degree, $D = b + c$, Sections 5.5 and 5.6 only
x, y, z	counts of v_0's appearances as hub, non-hub, leaf, respectively, across the t blocks, Section 5.6 only
k	v_0's total appearance count, $k = x + y + z$, Section 5.6 only; unrelated to the family index k of HS_{3k} used in Sections 1 and 2

Remark 8. *The tripartite necessary condition follows the same edge-count argument as the bipartite case (Proposition 3): since $|E(K_{a,b,c})| = ab + bc + ca$ and each HS_{12}-copy contributes 12 edges, $HS_{12} \mid K_{a,b,c}$ forces $12 \mid (ab + bc + ca)$.*

Write $q(a,b,c) = ab + bc + ca$. Since $12 = 4 \cdot 3$ with $\gcd(4,3) = 1$, the Chinese Remainder Theorem gives

$$12 \mid q(a,b,c) \iff 4 \mid q(a,b,c) \text{ and } 3 \mid q(a,b,c).$$

Let $k = \#\{x \in \{a,b,c\} : x \text{ odd}\}$. If $k \geq 2$, then some product in q is odd, while the other two have opposite parity contributions, whence $q \equiv 1 \pmod 2$ and $4 \nmid q$. If $k = 0$, then $4 \mid ab,\ bc,\ ca$ termwise. If $k = 1$, say a odd and $b = 2\beta$, $c = 2\gamma$, then

$$q \equiv bc \equiv 4\beta\gamma \equiv 0 \pmod 4 \iff b \equiv c \pmod 4,$$

the last equivalence following from $q = a(b+c) + bc$ and $b + c \equiv 0 \pmod 4$ exactly when $b \equiv c \pmod 4$ for b, c even. Hence,

$$4 \mid q(a,b,c) \iff \big(2 \mid a,\ 2 \mid b,\ 2 \mid c\big) \text{ or } \big(k = 1 \text{ and the two even entries agree mod } 4\big). \quad (4)$$

Modulo 3, reduce to $a', b', c' \in \mathbb{Z}_3$. If at least two of a', b', c' vanish, then every term of q carries a factor of 3; otherwise, $q \equiv a'b' + b'c' + c'a' \pmod 3$, and enumerating $\mathbb{Z}_3^3$ shows this vanishes precisely when $a' = b' = c'$. Hence,

$$3 \mid q(a,b,c) \iff \#\{x : 3 \mid x\} \geq 2 \text{ or } a \equiv b \equiv c \pmod 3. \quad (5)$$

Conditions (4) and (5) together are equivalent to $12 \mid q(a,b,c)$, and they are referred to below as (i) and (ii).

5.1. The Biclique Structure of $K_{a,b,c}$ and the Hub Method

Theorem 7 (Biclique partition number of $K_{a,b,c}$)**.** *For every $a, b, c \geq 1$, the minimum size of a biclique partition of $K_{a,b,c}$ is exactly 2, which is realised by one of the three hub decompositions $\{K_{X,Y\cup Z}, K_{Y,Z}\}$, $\{K_{Y,X\cup Z}, K_{X,Z}\}$, $\{K_{Z,X\cup Y}, K_{X,Y}\}$.*

Proof. No single biclique can equal $E(K_{a,b,c})$: a biclique's two sides cannot both meet the same part of $K_{a,b,c}$, so with three parts split between two sides, some pair of parts shares a side and the edges between them are missing. This gives the lower bound 2; each hub decomposition is readily checked to be a valid biclique partition of size 2, giving the upper bound. □

Corollary 5 (Hub sufficiency)**.** *If the hub-H condition (Definition 5) holds for some $H \in \{X, Y, Z\}$, then $HS_{12} \mid K_{a,b,c}$.*

Proof. By Theorem 7, the hub-H biclique partition splits $E(K_{a,b,c})$ edge-disjointly into a copy of $K_{|H|,|Q|+|R|}$ and a copy of $K_{|Q|,|R|}$; if the hub-H condition holds, Theorem 5 supplies an HS_{12}-decomposition of each, whose union decomposes $K_{a,b,c}$. □

Corollary 6 (Embedding-width obstruction)**.** *If $\min(a,b,c) < 4$, no hub condition holds for $K_{a,b,c}$, for any values of the other two parts.*

Proof. Say $a < 4$. Hub-X requires $HS_{12} \mid K_{a,b+c}$, which is impossible by Lemma 2 since $a < 4$. Hub-Y requires $HS_{12} \mid K_{a,c}$, which is impossible for the same reason; hub-Z requires $HS_{12} \mid K_{a,b}$, which is likewise impossible. Every hub choice fails on a sub-condition that is structurally unsatisfiable. □

Remark 9. *This does not mean $K_{a,b,c}$ itself is never HS_{12}-decomposable when a part is below 4—only that the hub method cannot certify it, since a single copy of HS_{12} embedded in a tripartite host is free to properly 3-colour its octagon across all three parts at once, which is a possibility no 2-biclique partition can see. Because HS_{12}'s bipartite embedding width is only 4 on the P-side (as opposed to the width the pendant-free class of a symmetric sunlet-type graph of the same order would carry), the obstruction of Corollary 6 bites only below* min $= 4$*, leaving a comparatively small region of the domain uncertified by the hub method alone.*

Lemma 9. *For any $a, b, c \geq 1$ and any splitting $c = c_1 + c_2$ with $c_1, c_2 \geq 0$,*

$$K_{a,b,c} = K_{a,b,c_1} \oplus K_{a+b,\,c_2},$$

the second summand being the complete bipartite graph between $X \cup Y$ and the peeled block of size c_2. The analogous splitting holds with the roles of a, b, c permuted.

Proof. Partition Z into Z_1 (size c_1) and Z_2 (size c_2). Every edge of $K_{a,b,c}$ has both endpoints in $X \cup Y \cup Z_1$ or one endpoint in Z_2 and the other in $X \cup Y$; these two cases partition $E(K_{a,b,c})$ exactly. □

Lemma 10. *If $HS_{12} \mid K_{a,b,c}$ and $a + b \geq 4$, then $HS_{12} \mid K_{a,b,c+12}$. The analogous statement holds for growing either of the other two parts by* 12 *under the corresponding sum condition.*

Proof. Apply Lemma 9 with $c_1 = c$, $c_2 = 12$: $K_{a,b,c+12} = K_{a,b,c} \oplus K_{a+b,12}$. The first summand is HS_{12}-decomposable by hypothesis; the second is HS_{12}-decomposable by the universal fact established in the proof of Theorem 4 ($HS_{12} \mid K_{x,12}$ for every integer $x \geq 4$), since $a + b \geq 4$. The union decomposes $K_{a,b,c+12}$. □

Remark 10. *This bridge is comparatively unrestrictive: only the* sum *of the two fixed parts need reach 4—a condition satisfied by essentially every triple of interest, including many with one very small part—because $HS_{12} \mid K_{x,12}$ was established for* every $x \geq 4$ *rather than merely for x above some larger width threshold.*

Corollary 7. *For $a, b, c \geq 1$, let $a_0, b_0, c_0 \in \{1, \ldots, 12\}$ be the representatives of a, b, c modulo 12 obtained by taking the usual residue in $\{0, \ldots, 11\}$ and replacing it with 12 whenever that residue is 0 (so that every representative is a positive part size, never a degenerate 0). If $HS_{12} \mid K_{a_0,b_0,c_0}$, and each pairwise sum among the eventual a, b, c never drops below 4 during the construction (automatic once $a_0, b_0, c_0 \geq 2$, say), then $HS_{12} \mid K_{a,b,c}$ for the entire matching residue class.*

Proof. Write $a = a_0 + 12i$, $b = b_0 + 12j$, $c = c_0 + 12k$ for $i, j, k \geq 0$. Apply Lemma 10 i times to grow $a_0 \to a$ (using $b_0 + c_0 \geq 4$, preserved as b, c only grow), j times to grow $b_0 \to b$, and k times to grow $c_0 \to c$; each application's sum-condition remains satisfied throughout since the parts involved only increase. □

5.2. Master Theorem for $\min(a, b, c) \geq 8$

When all three parts are ≥8, Theorem 4 applies to every bipartite piece the hub method could need, and condition (iii) of Theorem 5 (the $m = 6$ exceptional family) can never trigger, since every quantity involved—each original part, and each pairwise sum—is at least $8 > 6$. The hub-P condition therefore reduces to pure divisibility.

Corollary 8. *Let $a, b, c \geq 8$. The hub-P condition (for $P = A$, say, with $Q = B, R = C$) holds if and only if* $12 \mid bc$ *and* $12 \mid a(b + c)$.

Proof. The following is immediate from Theorem 5: since $b, c \geq 8$ and $a, b + c \geq 8$, condition (i) (widths) holds automatically and condition (iii) (the $m = 6$ family) is vacuous in both bipartite pieces, leaving only $12 \mid bc$ and $12 \mid a(b + c)$. □

Direct enumeration over residues modulo 12 (Lemma 10 lets us work entirely at the level of residues, exactly as in Corollary 7) identifies exactly 16 residue patterns (a, b, c) mod 12, up to permutation, satisfying the necessary condition of Remark 8 for which *no* hub choice is divisibility compatible in the sense of Theorem 8:

$$(1,4,4),\ (1,10,10),\ (2,2,2),\ (2,2,5),\ (2,2,8),\ (2,2,11),\ (2,8,8),$$
$$(4,4,4),\ (4,4,7),\ (4,4,10),\ (4,10,10),\ (5,8,8),\ (7,10,10),$$
$$(8,8,8),\ (8,8,11),\ (10,10,10).$$

Theorem 8 (Sixteen hub-incompatible patterns)**.** *Among the 52 residue triples* (a, b, c) mod 12, $0 \leq a \leq b \leq c \leq 11$, *satisfying* $12 \mid (ab + bc + ca)$, *exactly 16 (listed above) admit no divisibility-compatible hub choice. Nonetheless, every one of the sixteen representative instances—*$K_{8,8,8}$, $K_{8,8,11}$, $K_{14,8,8}$, $K_{10,10,10}$, $K_{17,8,8}$, $K_{13,10,10}$, $K_{14,14,14}$, $K_{14,14,17}$, $K_{14,14,8}$, $K_{14,14,11}$, $K_{16,16,16}$, $K_{16,16,19}$, $K_{16,16,10}$, $K_{16,10,10}$, $K_{19,10,10}$, *and* $K_{13,16,16}$*—realising each of the sixteen patterns at its minimal admissible part sizes* ≥ 8, *is nonetheless* HS_{12}*-decomposable; by an explicit non-hub construction, each vertex of which properly 3-colours the octagon of* HS_{12} *across all three parts.*

Proof. The enumeration is a finite check over 52 residue triples, which is verified by direct computation. For each of the sixteen representative instances, the theorem's claim is proved by exhibiting an explicit, finite collection of HS_{12}-blocks—the same standard of proof as Lemma 4—each independently re-verified by a program checking pairwise edge-disjointness and the exact coverage of $E(K_{a,b,c})$, sharing no code with whichever method produced the certificate.

As a representative illustration, the first block of the smallest instance, $K_{8,8,8}$ (16 blocks total, reproduced in full in Appendix B), is

$$H_1 = \begin{pmatrix} & Y_5 & & Z_5 & & X_4 & & Z_2 & \\ X_0 & Z_6 & Y_7 & Z_0 & Y_0 & Z_3 & Y_4 & Z_1 & X_0 \end{pmatrix}.$$

A direct check confirms this block properly 3-colours the octagon: hubs X_0, Y_7, Y_0, Y_4 and non-hubs Z_6, Z_0, Z_3, Z_1 alternate between two of the three parts with pendant leaves Y_5, Z_5, X_4, Z_2 drawn from whichever part is not already used at each hub—exactly the proper-3-colouring condition stated in the theorem. The remaining fifteen blocks of $K_{8,8,8}$, and all fifteen other instances, are of the identical explicit, independently re-verified form, which is given in full in Appendix B. By Corollary 7 (applicable since every part in all sixteen representatives is $\geq 8 \geq 2$), and each of the sixteen resolved patterns extends to its full matching residue class. □

Corollary 9. $HS_{12} \mid K_{a,b,c}$ *for every* $a, b, c \geq 8$ *satisfying* $12 \mid (ab + bc + ca)$, *with no exceptions: the sixteen hub-incompatible residue patterns of Theorem 8 are all realised by an explicit non-hub construction, and every other pattern is realised by the hub method of Theorem 8.*

Theorem 9. *Let* $a, b, c \geq 8$. *Then,* $HS_{12} \mid K_{a,b,c}$ *if and only if* $12 \mid (ab + bc + ca)$.

Proof. The necessity is Remark 8. For sufficiency, if the residue pattern (a, b, c) mod 12 is not one of the sixteen listed in Theorem 8, $HS_{12} \mid K_{a,b,c}$ is certified by Theorem 8 together with Corollary 5 for some hub choice; if it is one of the sixteen, $HS_{12} \mid K_{a,b,c}$ is certified

instead by Corollary 9. Together, these cover every residue pattern satisfying the necessary condition via the residue-reduction of Corollary 7 in each branch. □

5.3. Small Parts: An Illustrative Example

Below the embedding width, the hub method is structurally blocked (Corollary 6), yet direct, genuinely tripartite constructions can still succeed. We record the smallest fully symmetric instance.

Example 1 ($K_{4,4,4}$). *Take $a = b = c = 4$. The following is a necessity: $ab + bc + ca = 3 \times 16 = 48$, and $12 \mid 48$. The hub is structurally blocked for every choice: hub-X requires $HS_{12} \mid K_{4,8}$ (fails: $12 \mid 32$ is false, and in any case $3 \nmid 8$, so Theorem 3 excludes it) and, independently, $HS_{12} \mid K_{4,4}$ (fails outright: $\max(4,4) = 4 < 8$, violating Lemma 2). By symmetry, every hub choice fails on its $K_{4,4}$ sub-piece. An explicit 4-block decomposition (see Figure 5), found by the CP-SAT model of Section 7 and independently re-verified, is given in Appendix B.*

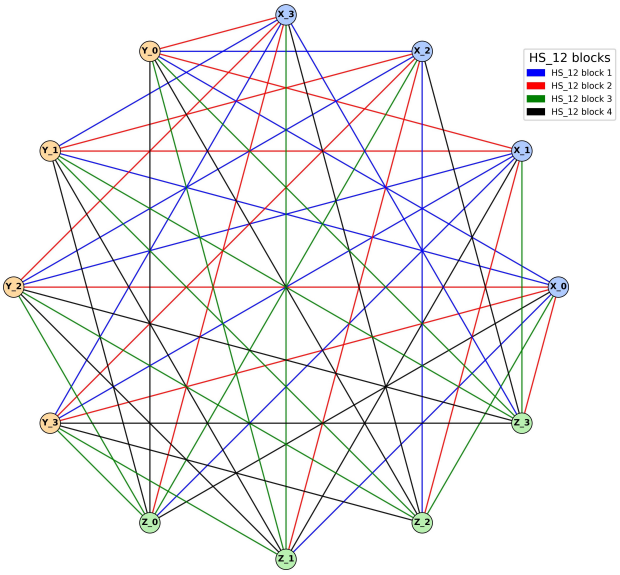


Figure 5. HS_{12}-decomposition of $K_{4,4,4}$.

Proposition 5 (Reducing the domain to a finite table). *Example 1 shows the phenomenon persists at HS_{12}'s own embedding width. Yet the domain $\min(a,b,c) < 8$, though infinite, reduces to a finite verification, as follows.*

(i) Residue-dependence. Write $a \leq 7$ for the smallest part (WLOG). Fixing a and writing $b = b_1 + 12i$, $c = c_1 + 12j$ for $b_1, c_1 \in \{0, \ldots, 11\}$, $i, j \geq 0$, direct expansion gives

$$ab + bc + ca = (ab_1 + b_1c_1 + ac_1) + 12\big(ai + b_1j + ic_1 + 12ij + aj\big),$$

so $ab + bc + ca \equiv ab_1 + b_1c_1 + ac_1 \pmod{12}$: the necessary condition $12 \mid (ab + bc + ca)$ depends on b, c only through their residues b_1, c_1; it does not depend on i, j.

(ii) Reduction to finitely many base cases. By (i) and Corollary 7, any single verified representative (a, b_1, c_1) extends to the entire matching residue class of b, c. So, every triple with $\min(a,b,c) < 8$ is governed by one of finitely many base cases (a, b_1, c_1), $1 \leq a \leq 7$, $b_1, c_1 \in \{0, \ldots, 11\}$.

(iii) Degenerate cases reduce to the bipartite theorem. If $b_1 = 0$ (i.e., $12 \mid b$), the repeated application of Lemma 9 (permuted to peel the b-part) splits $b = 12k$ into $K_{a,b,c} = K_{a,12,c} \oplus \underbrace{K_{a+c,12} \oplus \cdots \oplus K_{a+c,12}}_{k-1}$; each bipartite summand is settled by Theorem 5 directly, and the

tripartite remainder $K_{a,12,c}$ is settled by the hub-B choice of Corollary 5, whose two sub-conditions are $K_{12,a+c}$ (automatic, as 12 is never the exceptional value 6) and $K_{a,c}$ (again Theorem 5). So, $b_1 = 0$ (or symmetrically $c_1 = 0$) requires no new tripartite verification at all.

(iv) *Exact count. Excluding the degenerate cases by (iii), the remaining base cases are exactly the triples (a, b_1, c_1) with $1 \le a \le 7$, $1 \le b_1 \le c_1 \le 11$, satisfying $12 \mid (ab_1 + b_1c_1 + ac_1)$. Direct enumeration over this explicit, finite set of $7 \times \binom{11}{2}$-bounded candidates–an elementary divisibility check, not a decomposition search–gives exactly 41 such triples, 28 of which are distinct once a, b_1, c_1 are treated as an unordered set (i.e., once instances differing only by which of the three equal-role labels is called a are identified); every one of these 41 we resolve below.*

5.4. A Genuine Infinite Exceptional Family: $a = b = 2$

Unlike the isolated small exceptions of the $\min(a, b, c) \ge 8$ theory–each resolved by finding a single sufficiently large representative–the pair $a = b = 2$ produces a family that is exceptional for a structural reason independent of c.

Theorem 10 (The $(2, 2, c)$ obstruction)**.** *$HS_{12} \nmid K_{2,2,c}$ for every $c \ge 1$.*

Proof. Write A, B for the two size-2 parts and C for the third. Since $|A| = |B| = 2$, any embedding of a single copy of HS_{12} into $K_{2,2,c}$ assigns each of the twelve HS_{12}-vertices a colour in $\{A, B, C\}$ (its host part) subject to the following: (i) every HS_{12}-edge—each of the eight octagon edges and each of the four pendant edges—joins two differently coloured vertices (since $K_{2,2,c}$ has no edges within a part); and (ii) at most *two* vertices are coloured A and at most *two* are coloured B (there are only *two* actual vertices available in each part, and a single copy of HS_{12} cannot reuse a host vertex for two of its own vertices). There is no upper bound on how many vertices are coloured C.

We claim no admissible colouring realises an A-B edge. Let $\chi : V(HS_{12}) \to \{A, B, C\}$ satisfy (i) and (ii), and write $H = \{c_0, c_2, c_4, c_6\}$ for the hubs, $N = \{c_1, c_3, c_5, c_7\}$ for the non-hub cycle vertices and $L = \{p_0, p_2, p_4, p_6\}$ for the leaves, so that $V(HS_{12}) = H \sqcup N \sqcup L$ with $|H| = |N| = |L| = 4$. Put $\alpha = \chi^{-1}(A)$, $\beta = \chi^{-1}(B)$, so (ii) reads $|\alpha| \le 2$, $|\beta| \le 2$.

An exhaustive enumeration of the 3^{12} maps χ, retaining those satisfying (i)–(ii), returns exactly *six* colourings, which are characterised by

$$\alpha \cup \beta = H, \qquad |\alpha| = |\beta| = 2, \qquad \chi(N \cup L) = \{C\}, \tag{6}$$

i.e., the $\binom{4}{2} = 6$ ways of splitting the four hub slots between A and B. Indeed, any χ violating (6) fails (i)–(ii): if some $c_{2i} \in H$ has $\chi(c_{2i}) = C$, then its leaf p_{2i} needs a colour in $\{A, B\}$ by (i), and since $|\alpha| + |\beta| \le 4$ is already exhausted on H, this forces $|\alpha \cup \beta| > 4$, contradicting (ii); and if two adjacent vertices of the octagon both lie in $\alpha \cup \beta$, then the intervening non-hub must take the third colour, again by (i).

Under (6), every edge of HS_{12} has one endpoint in $H = \alpha \cup \beta$ and the other in $N \cup L \subseteq \chi^{-1}(C)$, since H is an independent set in the octagon and each leaf is adjacent only to its hub. Hence,

$$\chi(u) \ne A \ \text{ or } \ \chi(v) \ne B \qquad \text{for every } uv \in E(HS_{12}),$$

so no A-B edge occurs.

Since no single HS_{12}-block can contain an A-B edge, no decomposition of $K_{2,2,c}$, which requires covering all $ab = 4$ edges between A and B can exist for any c. □

Remark 11. *Theorem 10 is a genuine structural obstruction rather than a finite-representative artefact: the necessary condition of Remark 8 restricts c to $c \equiv 2 \pmod 3$ when $a = b = 2$, and we verified Theorem 10's conclusion computationally at representatives of all four resulting residues modulo 12 and at multiple scales within each ($c = 2, 5, 8, 11, 14, 17, 20, 23, 26$), which is consistent with the proof.*

Remark 12 (Why 2 specifically: the structural reason)**.** *The obstruction traces directly to HS_{12}'s own bipartition (Remark 2): hub positions c_0, c_2, c_4, c_6 are pairwise non-adjacent in the octagon, so* every *HS_{12}-edge joins a hub to a non-hub or a leaf—never hub to hub. An A-B edge can therefore only arise if one of A, B supplies non-hub/leaf vertices—but that role requires eight vertices (Lemma 2), which is far more than the two available in either part. Consequently, A, B can only ever supply hub–role vertices, between which no edge exists. This is not an artefact of $c = 2$ specifically: the same argument shows any part of size < 8 can never supply a non-hub/leaf role alongside a size-2 partner, so the obstruction is really a collision between the* smallest *possible part size and HS_{12}'s own larger bipartition class.*

5.5. A Second Infinite Exceptional Family: $a = 1, b = 4$

A structurally different obstruction, arising from a single vertex's own degree budget rather than a two-part supply cap, appears at $a = 1$, $b = 4$.

Lemma 11. *Let $a = 1$ and let $b, c \geq 1$ satisfy $12 \mid (b + bc + c)$. Write v_0 for the unique vertex of the singleton part, $D = b + c$ for its degree, and $t = (b + bc + c)/12$ for the number of blocks. In any single HS_{12}-block containing v_0, every edge incident to v_0 is unavailable to be a B-C edge (one endpoint is v_0 itself), so the number of B-C edges realised in that block is at most 12 minus v_0's degree contribution in that block (3 if v_0 is a hub, 2 if a non-hub cycle vertex, 1 if a leaf, 0 if absent). Summed over all t blocks, the total number of B-C edges realisable by any decomposition is at most $12t - D$. Since*

$$12t - D = (b + bc + c) - (b + c) = bc,$$

exactly the number of B-C edges required, every *block must realise its own individual maximum with no slack anywhere.*

Proof. The bound per block is immediate: v_0's own edges in that block are A-B or A-C, never B-C, so at most 12 minus that count can be B-C. Summing over blocks and using $\sum(v_0\text{'s degree contributions}) = D$ (every one of v_0's D edges is realised in exactly one block) gives the stated bound. The identity $12t - D = bc$ is direct algebra from the definitions of t and D. Since $K_{1,b,c}$ requires exactly bc B-C edges and the bound shows at most bc are achievable, equality is forced throughout. □

Theorem 11. *$HS_{12} \nmid K_{1,4,c}$ for every $c \equiv 4 \pmod{12}$.*

Proof. Write $c = 12m + 4$ for $m \geq 0$; direct computation gives $D = b + c = 12m + 8$ and $t = 5m + 2$. By Lemma 11, every block must realise its individual maximum B-C count. Exhaustive enumeration of the (at most) 3^{12} colourings of HS_{12}'s vertices with $\{A, B, C\}$, one vertex forced to A (namely v_0) and at most 4 to B, confirms this maximum equals exactly 12 minus v_0's degree-contribution in that block–9 if v_0 is a hub, 10 if a non-hub cycle vertex, 11 if a leaf, 12 if v_0 is absent–and identifies, for each of v_0's four possible roles, exactly which colourings attain it:

- v_0 absent (max 12): a unique colouring, up to the choice of which four vertices are B–namely, hub $= B$, everything else $= C$–since this is the only way to route every edge between a hub and a non-hub/leaf while both sides differ in colour.

- v_0 a leaf (max 11), or v_0 a non-hub cycle vertex (max 10): in both cases, exactly *four* colourings attain the maximum, one for each of v_0's *four* possible positions within that role, and in every one of them, all four hub positions are B.
- v_0 a hub (max 9): exactly *eight* colourings attain the maximum, *two* for each of v_0's *four* possible hub positions–one using all *four* B-vertices (the fourth as v_0's own pendant leaf), one using only *three* (with v_0's leaf coloured C)—and in every one of them, the *three* hub positions other than v_0's own are all B.

So whenever v_0 is not a hub, achieving the block's maximum forces all *four* hub positions to be B; whenever v_0 *is* a hub, it forces the remaining *three* to be B regardless of which of the two maximum-achieving configurations is used. Hence, if v_0 is a hub in exactly x of the t blocks, the total number of hub appearances forced onto the four B-vertices, summed over the whole decomposition, is exactly

$$3x + 4(t - x) = 4t - x.$$

This demand must be met by the four B-vertices' combined hub-appearance capacity. Each B-vertex has a degree of $1 + c = 12m + 5$, and each hub appearance costs it 3 of that degree, so no B-vertex can be a hub more than $\lfloor (12m + 5)/3 \rfloor = 4m + 1$ times; the four together supply at most $4(4m + 1) = 16m + 4$ hub appearances.

On the demand side, v_0's hub count x satisfies $3x \leq D$ (its hub appearances alone cannot exceed its total degree), so $x \leq \lfloor D/3 \rfloor = \lfloor (12m + 8)/3 \rfloor = 4m + 2$, giving demand

$$4t - x \;\geq\; 4t - (4m + 2) \;=\; 4(5m + 2) - (4m + 2) \;=\; 16m + 6.$$

Since $16m + 6 > 16m + 4$ for every $m \geq 0$, demand strictly exceeds supply regardless of how v_0's appearances are arranged across the t blocks. Hence, no decomposition exists. □

Remark 13 (Why $b = 4$ specifically: a degree threshold)**.** *With $a = 1$, each vertex of the third part has a degree of $a + b$. A hub role costs 3 of a vertex's degree, so supporting a* second *hub appearance requires a degree of ≥ 6. For $b \leq 4$, $a + b \leq 5 < 6$, capping every such vertex at one hub appearance ever; for $b \geq 5$, $a + b \geq 6$, relieving this cap entirely. Since $b = 1, 2, 3$ are not even arithmetically admissible with $a = 1$ (Section 3), $b = 4$ is the unique value at which the necessary condition $12 \mid (ab + bc + ca)$ holds* and *this degree cap binds—exactly the combination Lemma 11's demand-versus-supply argument exploits. This identifies $b = 4$ as a genuine boundary case rather than an arbitrary found value.*

5.6. Two Isolated Exceptions

Two further base cases fail at their minimal representative without belonging to an infinite family: unlike Theorems 10 and 11, a single larger instance in the same literal pair suffices to restore decomposability from that point onward.

Lemma 12 (Isolated exceptions)**.** *$HS_{12} \nmid K_{1,6,6}$ and $HS_{12} \nmid K_{2,3,6}$, but $HS_{12} \mid K_{1,6,c}$ for every $c \geq 18$ with $c \equiv 6 \pmod{12}$, and $HS_{12} \mid K_{2,3,c}$ for every $c \geq 18$ with $c \equiv 6 \pmod{12}$.*

Proof. The infeasibility of the two minimal instances, and the feasibility of $K_{1,6,18}$ (see Figure 6) and $K_{2,3,18}$ (see Figure 7), are established by direct CP-SAT construction and independent re-verification. Corollary 7, applied from the verified representatives $(1, 6, 18)$ and $(2, 3, 18)$ (each with all pairwise sums ≥ 4), extends feasibility to every larger $c \equiv 6 \pmod{12}$ in each family. □

Theorem 12 (Complete characterisation, $\min(a,b,c) < 8$)**.** *Let $a \le b \le c$ with $a < 8$ and $12 \mid (ab+bc+ca)$. Then, $HS_{12} \mid K_{a,b,c}$ if and only if $\{a,b,c\}$ is not one of the following:*

- $\{2,2,c\}$ *for any c (Theorem 10);*
- $\{1,4,c\}$ *for any $c \equiv 4 \pmod{12}$ (Theorem 11);*
- $\{1,6,6\}$ *or* $\{2,3,6\}$ *(Lemma 12).*

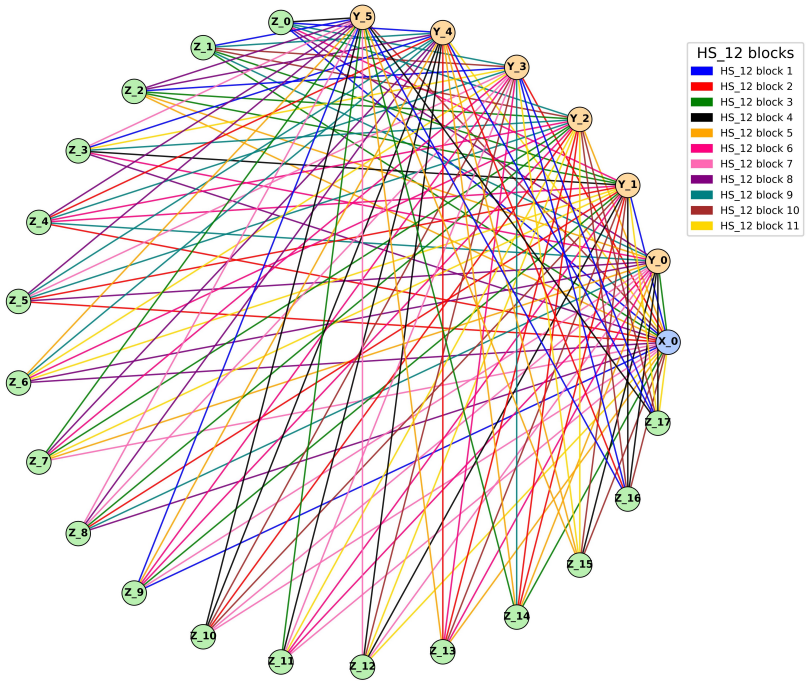


Figure 6. HS_{12}-decomposition of $K_{1,6,18}$.

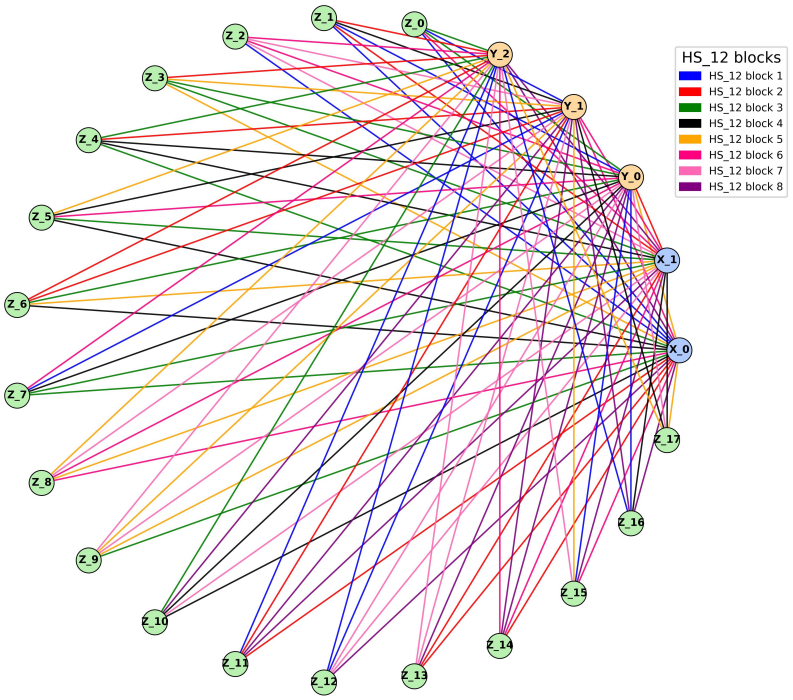


Figure 7. HS_{12}-decomposition of $K_{2,3,18}$.

Proof. The mathematical content of this theorem is the reduction itself (Proposition 5): every triple with $a < 8$ is governed, via Corollary 7's residue-class extension, by one of finitely many base representatives (a, b_1, c_1) with $a < 8$, $b_1, c_1 \in \{0, \ldots, 11\}$—an explicit,

finite reasoning step requiring no computation, reducing an infinite claim to 41 concrete instances. The degenerate cases ($b_1 = 0$ or $c_1 = 0$) are settled by Theorem 5 directly with no further exceptions. Of the remaining genuinely tripartite base cases, four are settled by the closed-form arguments of Theorems 10 and 11 and Lemma 12 (an exhaustive colouring argument, a degree-scheduling argument, and two isolated single-instance checks, respectively—none of these four uses certificate search at all). The remaining base cases are each positive instances, established, as in Lemma 4, by an explicit HS_{12}-block decomposition; every one is independently re-verified for pairwise edge-disjointness and exact edge coverage, and representative certificates are reproduced in Appendix C. Combining these four sources accounts for every one of the 41 base cases, and Corollary 7 extends each to its full residue class, giving the stated characterisation with no case left to computation alone. □

Remark 14. *Combined with Theorem 9 for* $\min(a,b,c) \geq 8$*, this gives a complete closed-form characterisation of* $HS_{12} \mid K_{a,b,c}$ *for* every *triple* $a,b,c \geq 1$*: the necessary condition* $12 \mid (ab+bc+ca)$ *is sufficient except for the two infinite families* $\{2,2,c\}$ *and* $\{1,4,c \ (c \equiv 4 \bmod 12)\}$ *and the two isolated triples* $\{1,6,6\}$, $\{2,3,6\}$*; all four exceptions were confined entirely to the domain* $\min(a,b,c) < 8$*.*

Remark 15 (Why the threshold is 8, and prospects for generalisation)**.** *The value 8 is not an artefact of the proof method but is forced by* HS_{12}*'s own structure: Lemma 2 shows any embedding of* HS_{12} *into a complete bipartite host requires the larger bipartition class* ($|Q| = 8$*) to be accommodated, so no argument—hub-based or otherwise—can avoid this threshold. In the tripartite hub method (Definition 5), a hub choice's harder sub-problem* $K_{|Q|,|R|}$ *falls into the delicate regime* $4 \leq \min(|Q|,|R|) < 8$ *precisely when some original part is* < 8*; Theorem 9's domain* $\min(a,b,c) \geq 8$ *is exactly where this can never happen for any hub choice, which is why it admits a uniform divisibility criterion while* $\min(a,b,c) < 8$ *(Theorem 12) instead requires the finite reduction of Proposition 5 together with the two infinite exceptional families. For the general half-sunlet family* HS_{3k}*, whose bipartition classes have sizes* k *and* $2k$ *(Section 2.1), the same reasoning predicts an analogous threshold at* $\min(a,b,c) \geq 2k$*, with the corresponding small-part regime* $k \leq a < 2k$ *requiring case-by-case treatment as it does here at* $k = 4$*; confirming this prediction for general* k *is a natural next step, which is discussed further in Section 8.*

6. A Formal Framework for Certificate-Based Decomposition

The results of Sections 3 and 5 rest on exhibiting explicit combinatorial witnesses. This section makes that notion fully precise independent of any particular search procedure used to produce one.

Definition 7 (Block placement)**.** *Let* G *be a complete bipartite or complete tripartite host graph on vertex set* $V(G)$*, which is partitioned into its parts. A* block placement *is an injective map* ϕ *from* HS_{12}*'s twelve labels* $c_0,\ldots,c_7,p_0,p_2,p_4,p_6$ *into* $V(G)$ *such that for every edge* uv *of* HS_{12}*,* $\phi(u)$ *and* $\phi(v)$ *lie in different parts of* G *(so* $\phi(u)\phi(v) \in E(G)$*). Write* $\phi(E(HS_{12})) = \{\phi(u)\phi(v) : uv \in E(HS_{12})\}$ *for the induced edge set, which is always a* 12*-element subset of* $E(G)$*.*

Definition 8 (Certificate)**.** *A* certificate *for* $HS_{12} \mid G$ *is a finite sequence of block placements* $\phi_1,\ldots,\phi_t$ *such that the following apply:*

(a) *(edge-disjointness)* $\phi_i(E(HS_{12})) \cap \phi_j(E(HS_{12})) = \emptyset$ *for all* $i \neq j$*;*
(b) *(exact coverage)* $\bigcup_{i=1}^{t} \phi_i(E(HS_{12})) = E(G)$*.*

Proposition 6 (Certificate existence is decomposability)**.** $HS_{12} \mid G$ *if and only if a certificate for* $HS_{12} \mid G$ *exists.*

Proof. It is immediate from Definitions 7 and 8, unpacking the definition of H-decomposability given in Section 1, that a partition of $E(G)$ into copies of HS_{12} is exactly a sequence of block placements satisfying (a)–(b), each $\langle \phi_i(E(HS_{12}))\rangle$ being isomorphic to HS_{12} by the construction of ϕ_i as an injective, edge-respecting map. □

Proposition 7 (Verification is mechanical)**.** *Given G and a candidate sequence $\phi_1, \ldots, \phi_t$, deciding whether it is a certificate (Definition 8) requires checking each ϕ_i's injectivity and part-respect ($O(1)$ per block, 12 labels), the pairwise edge-disjointness across all $\binom{t}{2}$ pairs of blocks ($O(t^2)$ set intersections on 12-element sets), and that the union equals $E(G)$ exactly ($O(t)$ once the edge count $12t = |E(G)|$ is confirmed by Proposition 3 or Remark 8). All three checks are polynomial in t and involve no search, no heuristic, and no dependence on how the candidate sequence was produced.*

By Proposition 6, proving $HS_{12} \mid G$ reduces to exhibiting one certificate; by Proposition 7, confirming that a given sequence is one is a fixed, mechanical procedure rather than a matter of trusting whatever method found it. The role of the computational methods described next (Section 7) is therefore solely to *search* the finite space of candidate block placements for one satisfying Definition 8 efficiently; the mathematical content—what must be found, and how a find is checked—is entirely specified above independent of CP-SAT or any other search procedure.

7. Computational Methodology and Verification

All certificates were produced with Google OR-Tools' CP-SAT solver [39] and independently re-verified. We record the models formally.

7.1. Models

Fix a host G with parts $V_1, \ldots, V_r$ ($r \in \{1, 2, 3\}$) and put $t = |E(G)|/12$. Index the twelve slots of HS_{12} by $S = \{c_0, \ldots, c_7, p_0, p_2, p_4, p_6\}$ and its edge set by $E(HS_{12})$ as in Definition 2. The decision variables are

$$\sigma_{b,s} \in V(G), \qquad b \in [t],\ s \in S,$$

assigning a host vertex to each slot of each block, subject to

$$\textsc{AllDifferent}\big(\sigma_{b,s} : s \in S\big), \qquad b \in [t], \tag{7}$$

$$\pi(\sigma_{b,u}) \neq \pi(\sigma_{b,v}), \qquad b \in [t],\ uv \in E(HS_{12}), \tag{8}$$

$$\textsc{AllDifferent}\big(\varepsilon(\sigma_{b,u}, \sigma_{b,v}) : b \in [t],\ uv \in E(HS_{12})\big), \tag{9}$$

where $\pi(x) = i$ iff $x \in V_i$ records the part of x, and $\varepsilon(x, y)$ is a fixed injective index of the unordered pair $\{x, y\}$. Constraint (7) makes each block a genuine embedding, (8) enforces that every HS_{12}-edge lands on an edge of G (vacuous when $r = 1$), and (9) forces the $12t = |E(G)|$ block-edges to be pairwise distinct, hence a bijection onto $E(G)$. A solution to (7)–(9) is therefore exactly a certificate in the sense of Definition 8.

7.2. Specialised Variants

Two refinements were needed where (7)–(9) alone proved intractable.

(i) *Hybrid greedy/exact.* For twelve of the sixteen patterns of Theorem 8 (block counts up to 72), blocks were placed sequentially by a randomised greedy rule preferring vertices of least residual degree; the residual edge set $R \subsetneq E(G)$ was then closed by solving (7)–(9) on R alone, under the symmetry-breaking constraints

$$\sigma_{b,c_0} = \min_{s \in S} \sigma_{b,s}, \qquad \sigma_{b,c_1} < \sigma_{b,c_7}, \qquad \sigma_{b,c_0} \leq \sigma_{b+1,c_0},$$

which quotient out the dihedral symmetry of the octagon and the ordering of blocks.

(ii) *Degree bounds.* Each hub role consumes exactly 3 of a vertex's degree budget, so writing h_v for the number of blocks in which v is a hub,

$$3h_v \le \deg_G(v) \quad \Longrightarrow \quad h_v \le \left\lfloor \tfrac{\deg_G(v)}{3} \right\rfloor.$$

Adding this valid inequality for every v resolved the $a = 1$ base cases underlying Theorem 11, which were otherwise out of reach.

7.3. Verification

Every certificate was re-checked by an independent routine sharing no code with the solver, which recomputes $\mathcal{E}_b = \{\{\sigma_{b,u}, \sigma_{b,v}\} : uv \in E(HS_{12})\}$ from the raw output and confirms

$$|\mathcal{E}_b| = 12 \ \ (b \in [t]), \qquad \mathcal{E}_b \cap \mathcal{E}_{b'} = \emptyset \ \ (b \neq b'), \qquad \bigcup_{b \in [t]} \mathcal{E}_b = E(G),$$

i.e., precisely conditions (a)–(b) of Definition 8. By Proposition 7, this check is polynomial and independent of how the candidate was found. All solver and verifier source code is provided in the Supplementary Information. No experimental, human-subject, or third-party data were used.

7.4. Choice of Solver Paradigm

All computations reported in this paper were carried out with the CP-SAT solver of Google OR-Tools, version `9.15.6755` [39], called through its Python interface. Problems (7)–(9) collectively demonstrate a pure satisfaction problem with no objective, and its constraints are AllDifferent predicates, which CP-SAT propagates natively. An ILP encoding of the same conditions requires auxiliary binaries and big-M linearisations that weaken propagation; unaided backtracking in Python `3.12.3` does not reach the largest instances here ($t \le 72$). General design-theory packages such as SageMath supply useful primitives but not the instance-specific symmetry-breaking and degree bounds above, which we imposed directly on the model. We did not run a formal comparative benchmark; a systematic comparison across paradigms remains open.

7.5. Computational Environment

Results were obtained with OR-Tools `9.15.6755` under Python `3.12.3` on an Intel Xeon processor at 2.10 GHz with 3 GB of available memory. Unless stated otherwise, solver calls used `num_search_workers` $= 8$ and a per-instance time limit of 300 s, with the random seed fixed at 1 so that the specific certificates reported here are reproducible. Two departures from these defaults were required and are noted where they occur: the largest complete-graph instance, K_{33} (44 blocks), was solved with `num_search_workers` $= 1$ to remain within available memory, and a small number of the harder tripartite instances required an extended time limit or a different seed. Per-certificate parameters are recorded in the Supplementary Information.

8. Conclusions and Future Work

For the half-sunlet graph HS_{12}, we have characterised the decomposability of all three complete host families, in each case proving the necessary edge-count condition sufficient up to an explicitly determined exception set $\mathcal{X}$:

$$
\begin{aligned}
HS_{12} \mid K_a &\iff a \geq 16,\ a \equiv 0,1,9,16 \pmod{24}; \quad \mathcal{X} = \emptyset,\\
HS_{12} \mid K_{a,b} &\iff m \geq 4,\ M \geq 8,\ 12 \mid ab; \quad \mathcal{X} = \{m = 6,\ 2 \mid M,\ 3 \nmid M\},\\
HS_{12} \mid K_{a,b,c} &\iff 12 \mid (ab + bc + ca); \quad \mathcal{X} = \big\{\{2,2,c\},\ \{1,4,c\}_{c\equiv 4 (12)},\ \{1,6,6\},\ \{2,3,6\}\big\},
\end{aligned}
$$

with $m = \min(a,b)$, $M = \max(a,b)$ (Theorems 6, 5, 9 and 12). Every tripartite exception is confined to $\min(a,b,c) < 8$. The three rows exhibit a structural gradient $|\mathcal{X}| = 0, 1, 4$: the vertex-transitive host imposes no width constraint and admits a purely arithmetic criterion, whereas HS_{12}'s asymmetric $4 + 8$ bipartition (Remark 2) produces obstructions as soon as the host's vertex classes are prescribed. Every sufficiency claim is backed by an explicit, independently re-verified certificate; no domain is left open. We also exhibited, in $K_{4,4,4}$, that the hub method's obstruction domain strictly contains the true non-decomposable set.

Three directions remain. First, the degree-scheduling mechanism behind Theorem 11 rests on the identity $12t - D = bc$ of Lemma 11, which is valid for *every* $a = 1$ instance; we conjecture it governs a general phenomenon.

Conjecture 1. *Let $a, b \geq 1$ be such that $12 \mid (ab + bc + ca)$ for infinitely many c. Then, the degree-scheduling comparison of Lemma 11, generalised to a part of size a, either exhibits an infinite exceptional family $\{a, b, c\}$ or certifies that none arises from this mechanism for the pair (a, b).*

The conjecture is consistent with both branches. For $a = 1$, $b \geq 5$, the bound $a + b \geq 6$ removes the single-hub cap that forces the deficit at $b = 4$, and every such base case in Appendix C is feasible. The boundary pair $(a, b) = (1, 6)$ shows the statement is sharp: no infinite family occurs, yet $K_{1,6,6}$ fails (Lemma 12) for reasons unrelated to degree scheduling, so isolated exceptions must still be checked separately.

Second, whether the analogous characterisations extend to HS_{3k} beyond $k = 4$ is open; Section 2.1 predicts a width threshold $\min \geq 2k$ in place of 8. Third, a systematic comparison of CP-SAT against ILP and general design-theory software on instances of this type would clarify how much of the observed scalability is attributable to the solver paradigm rather than to the problem-specific symmetry-breaking used here.

Supplementary Materials: The following supporting information can be downloaded at https://www.mdpi.com/article/10.3390/math14183354/s1, and it consists of a single Supplementary Information PDF document containing the full source code for every solver and independent verifier script used in this paper; complete detailed proofs, with independent computational corroboration, of Theorem 10 (the $K_{2,2,c}$ obstruction) and Theorem 11 (the $K_{1,4,c}$ obstruction), and a description of the accompanying JSON certificate data files.

Author Contributions: Conceptualization, G.P. and S.S.; methodology, G.P. and S.S.; formal analysis, G.P. and A.S.; investigation, G.P.; software, G.P.; validation, G.P. and A.S.; writing—original draft preparation, G.P.; writing—review and editing, S.S. and A.S.; supervision, A.S. The first and second authors originated the idea of extending HS_{12}-decomposition theory to complete bipartite and complete tripartite hosts, established and proved the core lemmas and theorems, worked out the explicit constructions and block certificates, carried out and verified the computational search, and wrote the initial manuscript draft. The second author directed the research programme; set the initial problem formulation and overall approach; oversaw the proof strategy at each stage; checked and validated all lemmas, theorems, and proofs for correctness; and reworked the manuscript's content, organisation, and presentation. All authors have read and agreed to the published version of the manuscript.

Funding: This research received no external funding.

Data Availability Statement: The certificate data, solver source code, and independent verifier scripts underlying every computational claim in this paper are provided in a Supplementary Information package accompanying this submission, and the block certificates themselves are additionally reproduced in full in Appendixes A–C.

Acknowledgments: We are grateful to PSG Institute of Technology and Applied Research, Tamil Nadu, India, for its continued support of this research.

Conflicts of Interest: The authors declare no conflicts of interest.

Appendix A. Bipartite Base-Case Certificates

This appendix documents the nine base bipartite decompositions underlying Theorems 3 and 4. Each certificate was found using the CP-SAT model of Section 7 and independently re-verified by a separate routine confirming the listed blocks are pairwise edge-disjoint copies of HS_{12} whose union is exactly the edge set of the stated graph. To keep this paper to a reasonable length, only one representative certificate is reproduced in full below in the matrix form of Definition 2 (bottom row: the host vertices assigned to the octagon $c_0, \ldots, c_7, c_0$ in cyclic order; top row, in the column immediately following each hub, the host vertex assigned to its pendant leaf; host vertices labelled X_i for the i-th vertex of the part of size a and Y_i for the i-th vertex of the part of size b, both 0-indexed). The remaining eight certificates are provided in full, in the same machine-readable and matrix-notation form, in the accompanying Supplementary Information.

Appendix A.1. Decomposition of $K_{4,9}$

$a = 4$, $b = 9$; $ab = 36$; 3 blocks.

$$H_1 = \begin{pmatrix} Y_3 & Y_5 & Y_7 & Y_2 \\ X_0\ Y_0\ X_1\ Y_1\ X_2\ Y_6\ X_3\ Y_8\ X_0 \end{pmatrix} \quad H_2 = \begin{pmatrix} Y_6 & Y_3 & Y_2 & Y_8 \\ X_0\ Y_1\ X_3\ Y_5\ X_2\ Y_4\ X_1\ Y_7\ X_0 \end{pmatrix}$$

$$H_3 = \begin{pmatrix} Y_5 & Y_6 & Y_8 & Y_7 \\ X_0\ Y_2\ X_1\ Y_3\ X_2\ Y_0\ X_3\ Y_4\ X_0 \end{pmatrix}$$

Appendix A.2. Decomposition of $K_{4,12}$

$a = 4$, $b = 12$; $ab = 48$; 4 blocks.

Full certificate (4 blocks) provided in the Supplementary Information (`cert_4_12.json`).

Appendix A.3. Decomposition of $K_{4,15}$

$a = 4$, $b = 15$; $ab = 60$; 5 blocks.

Full certificate (5 blocks) provided in the Supplementary Information (`cert_4_15.json`).

Appendix A.4. Decomposition of $K_{5,12}$

$a = 5$, $b = 12$; $ab = 60$; 5 blocks.

Full certificate (5 blocks) provided in the Supplementary Information (`cert_5_12.json`).

Appendix A.5. Decomposition of $K_{6,12}$

(See Figure 2) $a = 6$, $b = 12$; $ab = 72$; 6 blocks.

Full certificate (6 blocks) provided in the Supplementary Information (`cert_6_12.json`).

Appendix A.6. Decomposition of $K_{6,18}$

(See Figure 3) $a = 6$, $b = 18$; $ab = 108$; 9 blocks.

Full certificate (9 blocks) provided in the Supplementary Information (`cert_6_18.json`).

Appendix A.7. Decomposition of $K_{7,12}$

$a = 7$, $b = 12$; $ab = 84$; 7 blocks.

Full certificate (7 blocks) provided in the Supplementary Information (`cert_7_12.json`).

Appendix A.8. Decomposition of $K_{16,9}$

$a = 16$, $b = 9$; $ab = 144$; 12 blocks.

Full certificate (12 blocks) provided in the Supplementary Information (`cert_16_9.json`).

Appendix A.9. Decomposition of $K_{16,15}$

(See Figure 4) $a = 16$, $b = 15$; $ab = 240$; 20 blocks.

Full certificate (20 blocks) provided in the Supplementary Information (`cert_16_15.json`).

Appendix B. Tripartite Certificates

This appendix documents all sixteen tripartite decompositions realising the sixteen hub-incompatible residue patterns of Theorem 8 at their minimal admissible representative together with the small-part example $K_{4,4,4}$ (Example 1). Four instances ($K_{8,8,8}$, $K_{8,8,11}$, $K_{14,8,8}$, $K_{10,10,10}$) were found directly by the monolithic CP-SAT model of Section 7; the remaining twelve, whose block counts run up to 72, were found by the randomised sequential construction plus the exact residual solve described in Section 7. Every block, from either method, was independently re-verified by the same edge-cover check. To keep this paper to a reasonable length, only two representative certificates are reproduced in full below, which are in the same matrix form as Appendix A (host vertices labelled X_i, Y_i, Z_i for the parts of size a, b, and c, respectively): $K_{8,8,8}$, the canonical hub-incompatible pattern, and $K_{4,4,4}$, the small-part example of Example 1. The remaining fifteen certificates are provided in full in the accompanying Supplementary Information.

Appendix B.1. Decomposition of $K_{8,8,8}$

$a = 8$, $b = 8$, $c = 8$; $ab + bc + ca = 192$; 16 blocks.

$$H_1 = \begin{pmatrix} Y_5 & Z_5 & X_4 & Z_2 \\ X_0 & Z_6 & Y_7 & Z_0 & Y_0 & Z_3 & Y_4 & Z_1 & X_0 \end{pmatrix} \quad H_2 = \begin{pmatrix} Y_2 & Y_5 & X_7 & Y_4 \\ X_0 & Y_3 & Z_7 & Y_7 & Z_3 & Y_1 & Z_5 & Y_0 & X_0 \end{pmatrix}$$

$$H_3 = \begin{pmatrix} Z_7 & X_2 & Z_3 & Z_6 \\ X_0 & Y_7 & Z_4 & X_7 & Y_3 & Z_1 & Y_5 & Z_5 & X_0 \end{pmatrix} \quad H_4 = \begin{pmatrix} Z_0 & Y_1 & Y_7 & X_0 \\ X_1 & Y_2 & Z_7 & Y_0 & Z_1 & X_5 & Z_2 & Y_3 & X_1 \end{pmatrix}$$

$$H_5 = \begin{pmatrix} Z_7 & Y_0 & Y_1 & Y_2 \\ X_1 & Y_7 & Z_2 & Y_5 & X_4 & Y_3 & Z_0 & Y_6 & X_1 \end{pmatrix} \quad H_6 = \begin{pmatrix} Z_6 & Z_5 & Y_6 & Z_7 \\ X_1 & Z_2 & X_3 & Y_2 & X_4 & Z_1 & X_6 & Y_1 & X_1 \end{pmatrix}$$

$$H_7 = \begin{pmatrix} Z_3 & Z_7 & Y_4 & Y_7 \\ X_1 & Y_0 & X_5 & Y_1 & X_3 & Z_0 & X_7 & Z_1 & X_1 \end{pmatrix} \quad H_8 = \begin{pmatrix} Z_5 & Y_7 & Y_3 & Z_6 \\ X_1 & Y_4 & X_5 & Z_3 & X_6 & Z_2 & Y_2 & Z_4 & X_1 \end{pmatrix}$$

$$H_9 = \begin{pmatrix} Y_2 & Z_4 & Z_3 & Y_3 \\ X_2 & Y_0 & X_6 & Z_0 & X_0 & Y_6 & X_5 & Z_5 & X_2 \end{pmatrix} \quad H_{10} = \begin{pmatrix} Y_3 & Z_4 & Z_2 & X_3 \\ X_2 & Z_7 & X_4 & Y_4 & X_7 & Z_6 & Y_6 & Z_3 & X_2 \end{pmatrix}$$

$$H_{11} = \begin{pmatrix} Y_7 & X_0 & Z_7 & Z_5 \\ X_2 & Y_6 & Z_4 & Y_5 & X_3 & Z_3 & X_4 & Z_2 & X_2 \end{pmatrix} \quad H_{12} = \begin{pmatrix} Y_5 & X_0 & Y_3 & Z_0 \\ X_2 & Z_1 & Y_1 & Z_4 & X_3 & Y_7 & X_4 & Z_6 & X_2 \end{pmatrix}$$

$$H_{13} = \begin{pmatrix} Y_4 & Z_4 & Y_7 & Z_7 \\ X_2 & Z_0 & X_5 & Z_6 & X_6 & Z_5 & X_7 & Y_1 & X_2 \end{pmatrix} \quad H_{14} = \begin{pmatrix} Y_0 & Z_7 & Z_3 & Z_4 \\ X_3 & Z_1 & Y_6 & X_6 & Y_2 & Z_5 & Y_3 & Z_6 & X_3 \end{pmatrix}$$

$$H_{15} = \begin{pmatrix} Z_6 & Z_1 & Z_3 & Z_7 \\ Y_0 & X_7 & Y_2 & X_5 & Y_5 & Z_0 & Y_4 & Z_4 & Y_0 \end{pmatrix} \quad H_{16} = \begin{pmatrix} X_0 & X_1 & Z_5 & Z_0 \\ Y_4 & X_6 & Y_5 & X_7 & Y_6 & Z_2 & Y_1 & Z_6 & Y_4 \end{pmatrix}$$

Appendix B.2. Decomposition of $K_{8,8,11}$

$a = 8$, $b = 8$, $c = 11$; $ab + bc + ca = 240$; 20 blocks.

Full certificate (20 blocks) provided in the Supplementary Information (`tricert_8_8_11.json`).

Appendix B.3. Decomposition of $K_{14,8,8}$

$a = 14$, $b = 8$, $c = 8$; $ab + bc + ca = 288$; 24 blocks.

Full certificate (24 blocks) provided in the Supplementary Information (`tricert_14_8_8.json`).

Appendix B.4. Decomposition of $K_{10,10,10}$

$a = 10$, $b = 10$, $c = 10$; $ab + bc + ca = 300$; 25 blocks.

Full certificate (25 blocks) provided in the Supplementary Information (`tricert_10_10_10.json`).

Appendix B.5. Decomposition of $K_{17,8,8}$

$a = 17$, $b = 8$, $c = 8$; $ab + bc + ca = 336$; 28 blocks.

Full certificate (28 blocks) provided in the Supplementary Information (`tricert_17_8_8.json`).

Appendix B.6. Decomposition of $K_{13,10,10}$

$a = 13$, $b = 10$, $c = 10$; $ab + bc + ca = 360$; 30 blocks.

Full certificate (30 blocks) provided in the Supplementary Information (`tricert_13_10_10.json`).

Appendix B.7. Decomposition of $K_{14,14,14}$

$a = 14$, $b = 14$, $c = 14$; $ab + bc + ca = 588$; 49 blocks.

Full certificate (49 blocks) provided in the Supplementary Information (`tricert_14_14_14.json`).

Appendix B.8. Decomposition of $K_{14,14,17}$

$a = 14$, $b = 14$, $c = 17$; $ab + bc + ca = 672$; 56 blocks.

Full certificate (56 blocks) provided in the Supplementary Information (`tricert_14_14_17.json`).

Appendix B.9. Decomposition of $K_{14,14,8}$

$a = 14$, $b = 14$, $c = 8$; $ab + bc + ca = 420$; 35 blocks.

Full certificate (35 blocks) provided in the Supplementary Information (`tricert_14_14_8.json`).

Appendix B.10. Decomposition of $K_{14,14,11}$

$a = 14$, $b = 14$, $c = 11$; $ab + bc + ca = 504$; 42 blocks.

Full certificate (42 blocks) provided in the Supplementary Information (`tricert_14_14_11.json`).

Appendix B.11. Decomposition of $K_{16,16,16}$

$a = 16$, $b = 16$, $c = 16$; $ab + bc + ca = 768$; 64 blocks.

Full certificate (64 blocks) provided in the Supplementary Information (`tricert_16_16_16.json`).

Appendix B.12. Decomposition of $K_{16,16,19}$

$a = 16$, $b = 16$, $c = 19$; $ab + bc + ca = 864$; 72 blocks.

Full certificate (72 blocks) provided in the Supplementary Information (`tricert_16_16_19.json`).

Appendix B.13. Decomposition of $K_{16,16,10}$

$a = 16$, $b = 16$, $c = 10$; $ab + bc + ca = 576$; 48 blocks.

Full certificate (48 blocks) provided in the Supplementary Information (`tricert_16_16_10.json`).

Appendix B.14. Decomposition of $K_{16,10,10}$

$a = 16$, $b = 10$, $c = 10$; $ab + bc + ca = 420$; 35 blocks.

Full certificate (35 blocks) provided in the Supplementary Information (`tricert_16_10_10.json`).

Appendix B.15. Decomposition of $K_{19,10,10}$

$a = 19$, $b = 10$, $c = 10$; $ab + bc + ca = 480$; 40 blocks.

Full certificate (40 blocks) provided in the Supplementary Information (`tricert_19_10_10.json`).

Appendix B.16. Decomposition of $K_{13,16,16}$

$a = 13$, $b = 16$, $c = 16$; $ab + bc + ca = 672$; 56 blocks.

Full certificate (56 blocks) provided in the Supplementary Information (`tricert_13_16_16.json`).

Appendix B.17. Decomposition of $K_{4,4,4}$

(See Figure 5) $a = 4$, $b = 4$, $c = 4$; $ab + bc + ca = 48$; 4 blocks.

$$H_1 = \begin{pmatrix} Z_1 & Z_3 & Z_0 & Z_2 \\ X_0\ Y_1 & X_3\ Y_3 & X_1\ Y_2 & X_2\ Y_0\ X_0 \end{pmatrix} \quad H_2 = \begin{pmatrix} Z_1 & Z_3 & Z_0 & Z_2 \\ X_2\ Y_3 & X_0\ Y_2 & X_3\ Y_0 & X_1\ Y_1\ X_2 \end{pmatrix}$$

$$H_3 = \begin{pmatrix} X_3 & X_2 & X_0 & X_1 \\ Z_1\ Y_3 & Z_0\ Y_2 & Z_2\ Y_1 & Z_3\ Y_0\ Z_1 \end{pmatrix} \quad H_4 = \begin{pmatrix} X_3 & X_2 & X_1 & X_0 \\ Z_2\ Y_3 & Z_3\ Y_2 & Z_1\ Y_1 & Z_0\ Y_0\ Z_2 \end{pmatrix}$$

Appendix C. Tripartite Base-Table Certificates for $\min(a, b, c) < 8$

This appendix documents certificates for the twenty positive base cases of Theorem 12 not already covered by Appendix B together with the two isolation-witness certificates $K_{1,6,18}$ and $K_{2,3,18}$ underlying Lemma 12. All were found by the CP-SAT model of Section 7 and independently re-verified. To keep this paper to a reasonable length, only one representative certificate is reproduced in full below, which is in the same matrix form as Appendixes A and B: $K_{2,6,6}$, the smallest instance in this table. The remaining twenty-one certificates are provided in full in the accompanying Supplementary Information.

Appendix C.1. Decomposition of $K_{1,10,10}$

$a = 1$, $b = 10$, $c = 10$; $ab + bc + ca = 120$; 10 blocks.

Full certificate (10 blocks) provided in the Supplementary Information (`small_tricert_1_10_10.json`).

Appendix C.2. Decomposition of $K_{1,6,18}$

(See Figure 6) $a = 1$, $b = 6$, $c = 18$; $ab + bc + ca = 132$; 11 blocks.

Full certificate (11 blocks) provided in the Supplementary Information (`small_tricert_1_6_18.json`).

Appendix C.3. Decomposition of $K_{2,3,18}$

(See Figure 7) $a = 2$, $b = 3$, $c = 18$; $ab + bc + ca = 96$; 8 blocks.

Full certificate (8 blocks) provided in the Supplementary Information (`small_tricert_2_3_18.json`).

Appendix C.4. Decomposition of $K_{2,6,6}$

$a = 2, b = 6, c = 6$; $ab + bc + ca = 60$; 5 blocks.

$$H_1 = \begin{pmatrix} Y_3 & Z_5 & Z_1 & Y_0 \\ Z_3\ X_0\ Y_5 & Z_2\ Y_2\ X_1 & Z_0\ Y_1\ Z_3 \end{pmatrix} H_2 = \begin{pmatrix} Y_2 & Y_0 & Z_0 & Z_1 \\ Z_3\ Y_4\ Z_5 & Y_3\ X_0\ Y_1 & X_1\ Y_5\ Z_3 \end{pmatrix}$$

$$H_3 = \begin{pmatrix} Y_2 & Z_0 & Z_3 & Y_1 \\ Z_4\ X_0\ Y_4 & Z_2\ X_1\ Y_3 & Z_1\ Y_5\ Z_4 \end{pmatrix} H_4 = \begin{pmatrix} Y_1 & Z_2 & Z_5 & Y_5 \\ Z_4\ X_1\ Y_0 & Z_1\ X_0\ Y_2 & Z_0\ Y_3\ Z_4 \end{pmatrix}$$

$$H_5 = \begin{pmatrix} Y_2 & Z_1 & Z_3 & Y_3 \\ Z_5\ X_1\ Y_4 & Z_4\ Y_0\ X_0 & Z_2\ Y_1\ Z_5 \end{pmatrix}$$

Appendix C.5. Decomposition of $K_{2,6,9}$

$a = 2, b = 6, c = 9$; $ab + bc + ca = 84$; 7 blocks.

Full certificate (7 blocks) provided in the Supplementary Information (`small_tricert_2_6_9.json`).

Appendix C.6. Decomposition of $K_{2,8,8}$

$a = 2, b = 8, c = 8$; $ab + bc + ca = 96$; 8 blocks.

Full certificate (8 blocks) provided in the Supplementary Information (`small_tricert_2_8_8.json`).

Appendix C.7. Decomposition of $K_{3,6,6}$

$a = 3, b = 6, c = 6$; $ab + bc + ca = 72$; 6 blocks.

Full certificate (6 blocks) provided in the Supplementary Information (`small_tricert_3_6_6.json`).

Appendix C.8. Decomposition of $K_{3,6,10}$

$a = 3, b = 6, c = 10$; $ab + bc + ca = 108$; 9 blocks.

Full certificate (9 blocks) provided in the Supplementary Information (`small_tricert_3_6_10.json`).

Appendix C.9. Decomposition of $K_{4,4,7}$

$a = 4, b = 4, c = 7$; $ab + bc + ca = 72$; 6 blocks.

Full certificate (6 blocks) provided in the Supplementary Information (`small_tricert_4_4_7.json`).

Appendix C.10. Decomposition of $K_{4,4,10}$

$a = 4, b = 4, c = 10$; $ab + bc + ca = 96$; 8 blocks.

Full certificate (8 blocks) provided in the Supplementary Information (`small_tricert_4_4_10.json`).

Appendix C.11. Decomposition of $K_{4,6,6}$

$a = 4, b = 6, c = 6$; $ab + bc + ca = 84$; 7 blocks.

Full certificate (7 blocks) provided in the Supplementary Information (`small_tricert_4_6_6.json`).

Appendix C.12. Decomposition of $K_{4,10,10}$

$a = 4, b = 10, c = 10$; $ab + bc + ca = 180$; 15 blocks.

Full certificate (15 blocks) provided in the Supplementary Information (`small_tricert_4_10_10.json`).

Appendix C.13. Decomposition of $K_{5,6,6}$

$a = 5, b = 6, c = 6$; $ab + bc + ca = 96$; 8 blocks.

Full certificate (8 blocks) provided in the Supplementary Information (`small_tricert_5_6_6.json`).

Appendix C.14. Decomposition of $K_{5,8,8}$

$a = 5, b = 8, c = 8$; $ab + bc + ca = 144$; 12 blocks.

Full certificate (12 blocks) provided in the Supplementary Information (`small_tricert_5_8_8.json`).

Appendix C.15. Decomposition of $K_{6,6,6}$

$a = 6, b = 6, c = 6$; $ab + bc + ca = 108$; 9 blocks.

Full certificate (9 blocks) provided in the Supplementary Information (`small_tricert_6_6_6.json`).

Appendix C.16. Decomposition of $K_{6,6,7}$

$a = 6, b = 6, c = 7$; $ab + bc + ca = 120$; 10 blocks.

Full certificate (10 blocks) provided in the Supplementary Information (`small_tricert_6_6_7.json`).

Appendix C.17. Decomposition of $K_{6,6,8}$

$a = 6, b = 6, c = 8$; $ab + bc + ca = 132$; 11 blocks.

Full certificate (11 blocks) provided in the Supplementary Information (`small_tricert_6_6_8.json`).

Appendix C.18. Decomposition of $K_{6,6,9}$

$a = 6, b = 6, c = 9$; $ab + bc + ca = 144$; 12 blocks.

Full certificate (12 blocks) provided in the Supplementary Information (`small_tricert_6_6_9.json`).

Appendix C.19. Decomposition of $K_{6,6,10}$

$a = 6, b = 6, c = 10$; $ab + bc + ca = 156$; 13 blocks.

Full certificate (13 blocks) provided in the Supplementary Information (`small_tricert_6_6_10.json`).

Appendix C.20. Decomposition of $K_{6,6,11}$

$a = 6, b = 6, c = 11$; $ab + bc + ca = 168$; 14 blocks.

Full certificate (14 blocks) provided in the Supplementary Information (`small_tricert_6_6_11.json`).

Appendix C.21. Decomposition of $K_{6,9,10}$

$a = 6, b = 9, c = 10$; $ab + bc + ca = 204$; 17 blocks.

Full certificate (17 blocks) provided in the Supplementary Information (`small_tricert_6_9_10.json`).

Appendix C.22. Decomposition of $K_{7,10,10}$

$a = 7, b = 10, c = 10$; $ab + bc + ca = 240$; 20 blocks.

Full certificate (20 blocks) provided in the Supplementary Information (`small_tricert_7_10_10.json`).

References

1. Lindner, C.C.; Rodger, C.A. *Design Theory*, 2nd ed.; CRC Press: Boca Raton, FL, USA, 2009.
2. West, D.B. *Introduction to Graph Theory*, 2nd ed.; Prentice Hall: Upper Saddle River, NJ, USA, 2001.
3. Kirkman, T.P. On a problem in combinations. *Camb. Dublin Math. J.* **1847**, *2*, 191–204. [CrossRef]
4. Netto, E. Zur Theorie der Tripelsysteme. *Math. Ann.* **1893**, *42*, 143–152. [CrossRef]
5. Colbourn, C.J.; Rosa, A. *Triple Systems*; Oxford University Press: Oxford, UK, 1999.
6. Alspach, B.; Gavlas, H. Cycle decompositions of K_n and $K_n - I$. *J. Comb. Theory Ser. B* **2001**, *81*, 77–99.
7. Sajna, M. Cycle decompositions III: Complete graphs and fixed length cycles. *J. Comb. Des.* **2002**, *10*, 27–78. [CrossRef]
8. Bryant, D.; Horsley, D.; Pettersson, W. Cycle decompositions V: Complete graphs into cycles of arbitrary lengths. *Proc. Lond. Math. Soc.* **2014**, *108*, 1153–1192. [CrossRef]
9. Yamamoto, S.; Ikeda, H.; Shige-Eda, S.; Ushio, K.; Hamada, N. On claw-decomposition of complete graphs and complete bigraphs. *Hiroshima Math. J.* **1975**, *5*, 33–42. [CrossRef]
10. Ushio, K.; Tazawa, S.; Yamamoto, S. On claw-decomposition of a complete multipartite graph. *Hiroshima Math. J.* **1978**, *8*, 207–210. [CrossRef]
11. Tarsi, M. Decomposition of complete multigraphs into stars. *Discret. Math.* **1979**, *26*, 273–278. [CrossRef]
12. Lin, C.; Shyu, T.-W. A necessary and sufficient condition for the star decomposition of complete graphs. *J. Graph Theory* **1996**, *23*, 361–364. [CrossRef]
13. Jeevadoss, S.; Muthusamy, A. Decomposition of complete bipartite graphs into paths and cycles. *Discret. Math.* **2014**, *331*, 98–108. [CrossRef]
14. Bryant, D. Packing paths in complete graphs. *J. Comb. Theory Ser. B* **2010**, *100*, 206–215. [CrossRef]
15. Shyu, T.-W. Decomposition of complete graphs into paths and stars. *Discret. Math.* **2010**, *310*, 2164–2169. [CrossRef]
16. Shyu, T.-W. Decomposition of complete graphs into cycles and stars. *Graphs Comb.* **2013**, *29*, 301–313. [CrossRef]
17. Lonc, Z. Decompositions of graphs into trees. *J. Graph Theory* **1989**, *13*, 393–403. [CrossRef]
18. Sethuraman, G.; Murugan, V. Decomposition of complete graphs into arbitrary trees. *Graphs Comb.* **2021**, *37*, 1191–1203. [CrossRef]
19. Graham, R.L.; Pollak, H.O. On the addressing problem for loop switching. *Bell Syst. Tech. J.* **1971**, *50*, 2495–2519. [CrossRef]
20. Sotteau, D. Decomposition of $K_{m,n}$ ($K^*_{m,n}$) into cycles (circuits) of length $2k$. *J. Comb. Theory Ser. B* **1981**, *30*, 75–81. [CrossRef]
21. Chou, C.C.; Fu, C.M.; Huang, W.C. Decomposition of $K_{m,n}$ into short cycles. *Discret. Math.* **1999**, *197/198*, 195–203. [CrossRef]
22. Chou, C.C.; Fu, C.M. Decomposition of $K_{m,n}$ into 4-cycles and $2t$-cycles. *J. Comb. Optim.* **2007**, *14*, 205–218. [CrossRef]
23. Tarsi, M. Decomposition of complete multigraph into simple paths: Nonbalanced handcuffed designs. *J. Comb. Theory Ser. A* **1983**, *34*, 60–70. [CrossRef]
24. Shyu, T.-W. Decomposition of complete bipartite graphs into paths and stars with the same number of edges. *Discret. Math.* **2013**, *313*, 865–871. [CrossRef]
25. Lee, H.-C. Decomposition of the complete bipartite multigraph into cycles and stars. *Discret. Math.* **2015**, *338*, 1362–1369. [CrossRef]
26. Lee, H.-C.; Chu, Y.-P. Multidecompositions of the balanced complete bipartite graph into paths and stars. *ISRN Comb.* **2013**, *2013*, 727218. [CrossRef]
27. Anitha, R.; Lekshmi, R.S. N-sun decomposition of complete graphs and complete bipartite graphs. *World Acad. Sci. Eng. Technol.* **2007**, *27*, 262–266.
28. Anitha, R.; Lekshmi, R.S. N-sun decomposition of complete, complete bipartite and some Harary graphs. *Int. J. Comput. Math. Sci.* **2008**, *2*, 33–38.
29. Fu, C.M.; Jhuang, N.H.; Lin, Y.L.; Sung, H.M. On the existence of k-sun systems. *Discret. Math.* **2012**, *312*, 1931–1939. [CrossRef]
30. Fu, C.M.; Huang, M.H.; Lin, Y.L. On the existence of 5-sun systems. *Discret. Math.* **2013**, *313*, 2942–2950. [CrossRef]
31. Cavenagh, N.J. Decompositions of complete tripartite graphs into k-cycles. *Australas. J. Comb.* **1998**, *18*, 193–200.
32. Billington, E.J. Decomposing complete tripartite graphs into cycles of lengths 3 and 4. *Discret. Math.* **1999**, *197/198*, 123–135. [CrossRef]
33. Ganesamurthy, S.; Paulraja, P. Decompositions of complete tripartite graphs into cycles of lengths 3 and 6. *Australas. J. Comb.* **2019**, *73*, 220–241.
34. Mahmoodian, E.S.; Mirzakhani, M. Decomposition of complete tripartite graphs into 5-cycles. In *Combinatorics Advances*; Colbourn, C.J., Mahmoodian, E.S., Eds.; Kluwer Academic Publishers: Dordrecht, The Netherlands, 1995; pp. 235–241.
35. Cavenagh, N.J.; Billington, E.J. On decomposing complete tripartite graphs into 5-cycles. *Australas. J. Comb.* **2000**, *22*, 41–62.
36. Alipour, S.; Mahmoodian, E.S.; Mollaahmadi, E. On decomposing complete tripartite graphs into 5-cycles. *Australas. J. Comb.* **2012**, *54*, 289–301.
37. Priyadharsini, S.; Shanmugasundaram, S.; Muthusamy, A. Decomposition of complete tripartite graphs into cycles and paths of length three. *Contrib. Discret. Math.* **2020**, *15*, 117–129. [CrossRef]

38. Billington, E.J.; Cavenagh, N.J.; Smith, B.R. Path and cycle decompositions of complete equipartite graphs: 3 and 5 parts. *Discret. Math.* **2010**, *310*, 241–252. [CrossRef]
39. Perron, L.; Didier, F. CP-SAT Solver, Google OR-Tools, Version `9.15.6755`. Available online: https://developers.google.com/optimization/cp/cp_solver/ (accessed on 1 August 2026).
40. Sonawane, A.V.; Borse, Y.M. Decomposition of hypercubes into sunlet graphs of order eight. *Discret. Math. Algorithms Appl.* **2021**, *13*, 2150123. [CrossRef]
41. Sowndhariya, K.; Muthusamy, A. Decomposition of product graphs into sunlet graphs of order eight. *J. Algebra Comb. Discret. Appl.* **2021**, *8*, 41–51. [CrossRef]
42. Ezhilarasi, A.P.; Muthusamy, A. Decomposition of complete equipartite graphs into path and cycle of size $2p$. *Discret. Math.* **2023**, *346*, 113164. [CrossRef]
43. Priyadarsini, S. Decomposition of complete tripartite graphs into cycles and paths of length k. *Ann. Pure Appl. Math.* **2023**, *28*, 35–41. [CrossRef]
44. Arputha Jose, T.; Sampath Kumar, S.; Cecily Sahai, C. Decomposition of complete tripartite graphs into short cycles. *Ars. Comb.* **2024**, *160*, 85–103. [CrossRef]
45. Saranya, D.; Jeevadoss, S.; Nalini, V.; Chitra, V. Decomposition of hypercube graphs into paths and cycles having k edges. *AKCE Int. J. Graphs Comb.* **2025**, *22*, 190–195. [CrossRef]
46. Nalini, V.; Jeevadoss, S. Decomposition of regular bipartite graphs into Hamiltonian cycles (paths) and S_3. *J. Math.* **2025**, *2025*, 2349979. [CrossRef]
47. Oyewumi, O.; Akwu, A.; Azer, T. Path Decomposition Number of Certain Graphs. *Open J. Discret. Appl. Math.* **2018**, *1*, 26–32. [CrossRef]

Disclaimer/Publisher's Note: The statements, opinions and data contained in all publications are solely those of the individual author(s) and contributor(s) and not of MDPI and/or the editor(s). MDPI and/or the editor(s) disclaim responsibility for any injury to people or property resulting from any ideas, methods, instructions or products referred to in the content.